University of Nebraska - Lincoln
DigitalCommons@University of Nebraska - Lincoln

Dissertations, Theses, & Student Research in Food Science and Technology

Food Science and Technology Department

12-2012

Characterization of Starch by Vibrational Spectroscopy

Brandon H. Holder
University of Nebraska–Lincoln, bh.holder@gmail.com

Follow this and additional works at: https://digitalcommons.unl.edu/foodscidiss

 Part of the Food Science Commons

Holder, Brandon H., "Characterization of Starch by Vibrational Spectroscopy" (2012). *Dissertations, Theses, & Student Research in Food Science and Technology*. 27.
https://digitalcommons.unl.edu/foodscidiss/27

This Article is brought to you for free and open access by the Food Science and Technology Department at DigitalCommons@University of Nebraska - Lincoln. It has been accepted for inclusion in Dissertations, Theses, & Student Research in Food Science and Technology by an authorized administrator of DigitalCommons@University of Nebraska - Lincoln.

CHARACTERIZATION OF STARCH
BY VIBRATIONAL SPECTROSCOPY

by

Brandon H. Holder

A THESIS

Presented to the Faculty of

The Graduate College at the University of Nebraska

In Partial Fulfillment of Requirements

For the Degree of Master of Science

Major: Food Science & Technology

Under the Supervision of Professor Randy L. Wehling

Lincoln, Nebraska

December, 2012

CHARACTERIZATION OF STARCH BY VIBRATIONAL SPECTROSCOPY

Brandon Holder, M.S.
University of Nebraska, 2012
Advisor: Randy Wehling

To develop a dispersive Raman spectroscopic method for measuring amylose-amylopectin ratios of corn starch mixtures, 67 mixtures were prepared by randomly mixing waxy and normal corn starches. Amylose contents were measured using a dual wavelength iodine binding colorimetric method. Raman data were collected from 250 to 3200 cm^{-1} using optimized instrument parameters. Partial least-squares (PLS) and principal components regression (PCR) were used to prepare multivariate calibration models; however, PLS commonly outperformed PCR. Truncating the spectra to 250 to 2000 cm^{-1} improved the results (r^2 of validation = 0.831, SEP = 2.90%). Removal of a cold water swelling starch from the data also offered a slight improvement in results (r^2 of validation = 0.860, SEP = 2.70%). Dispersive Raman spectroscopy may not be well suited for quantifying amylose content of starch mixtures; however, the method was easily capable of discriminating between waxy and normal starches. This may allow the method to be used for confirming the identity of starch shipments.

A dispersive Raman spectroscopic method for measuring retrogradation in corn starch gels was investigated. Thirty-six gels were prepared, stored at 4° C and measured at regular time intervals (0 h, 24 h, 48 h, 72 h, 120 h, 168 h after preparation). After each measurement, the gels were freeze-dried, then each resultant dried gel was ground into a powder and measured using X-ray diffraction. Relative crystallinity was determined, and intensity changes in the Raman band at 480 cm^{-1} were measured. No correlation was

found between changes in the 480 cm^{-1} band and the relative crystallinity of the gels (r^2 < .1). The low starch concentration used may have caused the poor Raman signal strength and the unpredictable changes in the X-ray diffraction data. The experiment found that measuring retrogradation in very dilute starch gels could be problematic, and that more development is needed in order to apply Raman spectroscopy to in a food system like white pan bread.

DEDICATION

I would like to dedicate this thesis to my wife, Erin, and my mother, Mary, who have been enormous pillars of support throughout my graduate school experience. I would also like to extend this dedication to my grandmother and grandfather, Mary and Tyrone, who taught me the unwavering value of education.

ACKNOWLEDGEMENT

I would like to thank Dr. Randy Wehling for offering me the tremendous opportunity of coming to University of Nebraska and studying under him. In addition, I would like to thank him for all of his advice and support with regard to the experiments and problems that arose during the study. Also, I would like to thank my committee members, Dr. Jeyamkondan Subbiah and Dr. Susan Cuppett, who offered guidance and advice as well over the course of the studies.

I would like to thank Dr. Devin Rose and Mr. Steve Weir of UNL's Food Processing Center, who provided starch samples for use in all of the experiments. I would also like to further thank Dr. Devin Rose and Dr. Wajira Ratnayake for allowing me the use of their equipment.

I would like to recognize the contributions of Dr. Wajira Ratnayake for his advice and guidance in how best to approach the starch retrogradation experiment and for his assistance in troubleshooting procedural problems with the iodine binding reference method. I would also like to extend thanks to Dr. Shah Valloppilly from the Physics & Astronomy Department at UNL for his assistance and training in collecting the X-ray diffraction data for the starch retrogradation experiment.

Finally, I would like to extend my appreciation to my friends – Sely Prajitna, Nyambe Mkandawire, Michelle Hoffman, Tara Stiles, Malcond Valladares and several others – who have been enormously helpful with their advice and care through my time at UNL.

TABLE OF CONTENTS

ABSTRACT i

DEDICATION iii

ACKNOWLEDGEMENT iv

LIST OF TABLES vii

LIST OF FIGURES viii

INTRODUCTION 1

CHAPTER I: Literature Review

Starch, Its Functional Properties and Quality Parameters 5

Methods for Measuring Amylose-Amylopectin Ratios 9

Overview of Vibrational and Raman Spectroscopy 12

Raman Spectrum of Starch and Band Assignments 14

Use of Raman Spectroscopy to Measure Amylose-Amylopectin Ratios 17

Methods for Measuring Retrogradation in Starch 19

Use of Raman Spectroscopy to Measure Retrogradation 23

References 27

CHAPTER II: Development of a Raman spectroscopic method for measuring amylose-amylopectin ratios of corn starch

Abstract 34

Introduction 35

Materials & Methods 37

- Corn starch mixture preparation 37
- Sample preparation for Raman spectroscopy 38
- Raman spectroscopy 38
- Spectral collection optimization 39
- Reference analysis 40
- Data preprocessing and chemometrics 41

Results & Discussion 43

Conclusions 53
References 55

CHAPTER III: Development of a Raman spectroscopic method for measuring retrogradation in corn starch gels

Abstract 58
Introduction 59
Materials and Methods 62
Sample preparation 62
Preparation of amorphous phase standards 63
Raman spectroscopy 64
Sample preparation for X-ray diffraction 65
X-ray diffraction 65
Spectral preprocessing and data analysis 67
Results and Discussion 67
Conclusions 77
References 78

SUMMARY 80

APPENDIX 82

LIST OF TABLES

CHAPTER I

Table 1.1. Examples of starch uses in various food industry products……....7

Table 1.2. Raman bands seen in starch and their vibrational mode assignments as reported in the literature…….16

CHAPTER II

Table 2.1. Summary statistics of the calibration and validation datasets including all 67 samples that met precision standards……....46

Table 2.2. Calibration model results of the calibration set detailed in Table 2.1……..47

Table 2.3. Validation results of the PLS calibration models from Table 2.2…..…….....48

Table 2.4. Summary statistics of the calibration and validation datasets excluding the cold water swelling starch, NOVATION 4600…….....52

Table 2.5. Calibration model results of the validation set detailed in Table 2.4……...53

Table 2.6. Best validation results for calibration models detailed in Table 2.5…...…….53

APPENDIX

Table A.1. Mixing protocol for preparation of corn starch mixtures…….82

Table A.2. Summary of blend codes used for preparation of normal and waxy corn starch mixtures……..84

Table A.3. Classifications and suggested analytical applications of a model based on the ratio of the standard error of prediction to the standard deviation of the validation data…….84

LIST OF FIGURES

CHAPTER I

Figure 1.1. General structure of amylose…….5

Figure 1.2. General structure of amylopectin……..6

Figure 1.3. Example FT-Raman spectra of corn starch (A) and cassava starch (B) collected using 1064 nm excitation……15

CHAPTER II

Figure 2.1. Example of the typical Raman spectrum of Argo normal corn starch collected using 785 nm (near-infrared) excitation……44

Figure 2.2. Plot of the instrument-predicted amylose content (2000 to 250 cm^{-1}) vs. the reference amylose content determined by iodine binding colorimetry……..49

Figure 2.3. Plot of the instrument-predicted amylose content (1500 to 250 cm^{-1}) vs. the reference amylose content determined by iodine binding colorimetry……..49

CHAPTER III

Figure 3.1. Raman spectrum between 3200 and 250 cm^{-1} of gelatinized Argo corn starch cooled for 45 min (t = 0 h) after cooking for 90 min…….....70

Figure 3.2. Plot comparing relative crystallinity with storage time in hours for one gel series prepared from Argo corn starch……...72

Figure 3.3. Plot comparing estimated relative crystallinity with storage time in hours for one gel series prepared from Argo corn starch…….....72

Figure 3.4. Diffractogram comparison of data from one gel series to the amorphous standard sample that was prepared…….....73

Figure 3.5. Comparison of Raman spectral data from a gel series prepared from Argo corn starch……..76

INTRODUCTION

Starch plays a crucial role in the food industry as a food ingredient. For example, more than 250 million bushels of corn were used in starch production in 2010, and an estimated 20 billion pounds of bread are produced yearly, a product in which wheat starch is a principal constituent (Zobel and Kulp 1996; USDA Economic Research Service 2010). In spite of the considerable market share that starches represent, quality measures for key attributes of starch and starch-containing products are often inefficient, imprecise and costly for food manufacturers. Vibrational spectroscopic techniques like Raman spectroscopy could offer an alternative to traditional quality measurements.

Amylose-amylopectin ratios of starches, a key quality consideration, appear to play a role in determining expansion properties of extruded products, can impact multiple quality characteristics of baked breads, and greatly influence important functional properties of starch like the ability to form pastes or gels (Chinnaswamy and Hanna 1988; Jane et al 1999; Johnson et al 1999; Lee et al 2001). Traditionally, amylose is quantified by wet chemical techniques like colorimetric determination using iodine. However, many of these early wet chemical techniques suffered from potential inaccuracies inherent to the methodology (Wang et al 1998; Zhu et al 2008). Additionally, both older and newer wet chemical techniques are often uneconomical, while some may require well-trained technicians to yield reproducible results (Zhu et al 2008). Bearing in mind these considerations, manufacturers have some incentive to explore other routes to obtain the same information. And yet, despite fairly extensive research examining related techniques like near-infrared reflectance spectroscopy, using Raman spectroscopy for this

purpose has never been particularly well researched. With increased emphasis by food manufacturers on both rapid and non-destructive quality testing, Raman spectroscopic determination of amylose-amylopectin ratios could present a valuable tool for starch producers, as the method would meet both criteria. Raman spectroscopy may also be helpful in overcoming another difficult challenge in quality testing: predicting quality changes related to retrogradation in starch-containing products.

Retrogradation is a primary cause of quality deterioration in starch-based food products and is generally implicated as the principal mechanism involved in staling of cereal products. Starch retrogradation is the process by which gelatinized starch, when cooled and aged, regains a degree of crystalline order by the re-association of starch's component polymers, first amylose and eventually amylopectin (Zobel and Kulp 1996). Resulting effects of this process are both an increase in firmness and a loss of moisture, quality changes that are in part associated with the return of about 600 million pounds of bread each year (Zobel and Kulp 1996). Although numerous techniques are available for monitoring starch retrogradation, few methods are available which offer the portability and rapid, non-destructive analysis of which Raman spectroscopy is capable (Viereck et al 2009). With an increased industry emphasis on such technologies, Raman spectroscopy may offer a practical approach to tackling the issue of monitoring retrogradation in starch-containing products. Furthermore, little research is available on using Raman spectroscopy to monitor starch retrogradation in gels, and few or no studies have been published on using Raman spectroscopy to monitor retrogradation in a model food product like white pan bread.

This research investigates the feasibility of alternative methods for monitoring important quality characteristics of starches and starch-containing products, an area of the food industry that is hugely important but lacks efficient and cost-effective quality measures. Furthermore, Raman spectroscopic techniques for monitoring these quality attributes offer a greener alternative to wet chemical methods, more portability in setting up quality testing with the possibility for on-line analysis applications, and potentially lower operating expense associated with purchasing and handling of costly chemical reagents for use in wet chemical testing.

The objective of this research was to develop and, when applicable, validate two analytical methods that use Raman spectroscopy to monitor quality traits of cereal starches and starch-containing products. The two major project-specific objectives of this research were:

- To develop, optimize, validate and evaluate the efficacy of an inexpensive Raman spectroscopic method for quantifying amylose-amylopectin ratios in corn starch.
- To develop and assess the usefulness of an inexpensive Raman spectroscopic method for continuous measurement of retrogradation in corn starch gels.

Chapter I:
LITERATURE REVIEW

Starch, Its Functional Properties and Quality Parameters

Starch is an energy storage polysaccharide found in plants that is composed of both a mostly linear and a highly branched polymer, amylose and amylopectin, respectively. Each polymer is comprised of D-glucose; the primary difference between them is in their linkages (Karim et al 2000). Shown in **Figure 1.1**, amylose's subunits are linked mostly α-(1→4). Amylopectin, displayed in **Figure 1.2**, has subunits linked both α-(1→4) and α-(1→6), with about 95% of the glycosidic bonds being α-(1→4) linkages and roughly 5% being α-(1→6) (Hoseney 1998). The α-(1→6) linkages in amylopectin cause the polymer to be highly branched (Karim et al 2000). These structural characteristics of starch's component polymers give rise to many unique functional properties that the food industry utilizes.

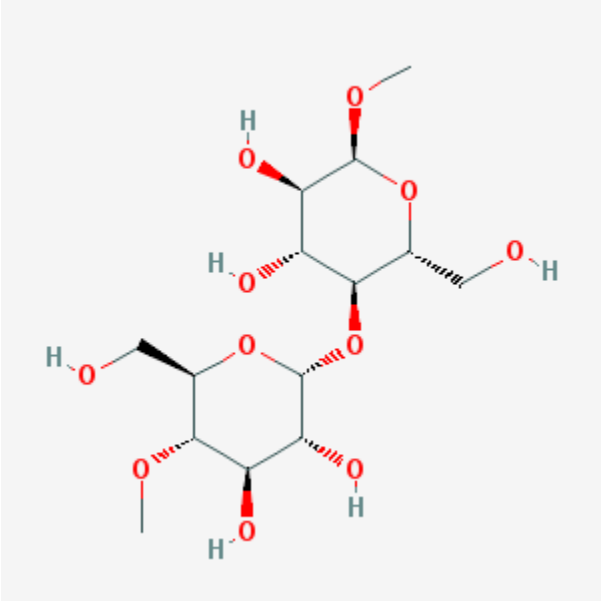

Figure 1.1: General structure of amylose (NCBI 2011).

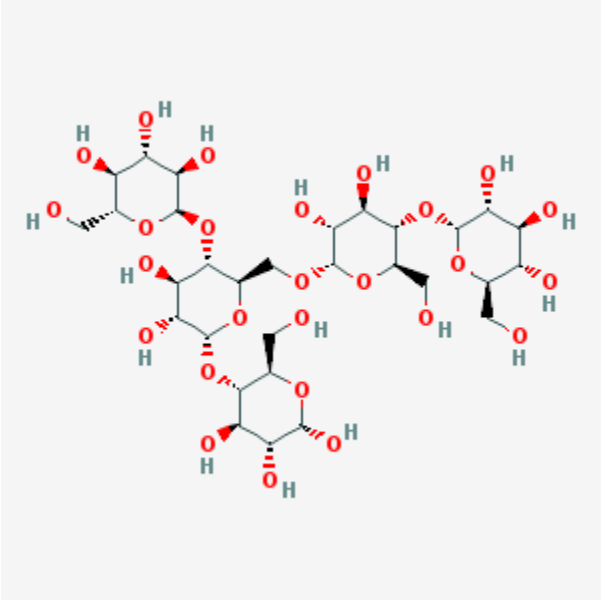

Figure 1.2: General structure of amylopectin (NCBI 2005).

The food industry uses modified and normal starches, particularly from maize, in a variety of products and processes such as: brewing, production of sauces and dressings, canned foods, and certain food mixes like instant puddings (Johnson et al 1999). Moreover, the majority of bakery products contain starch as a portion of the flour from which they are made, with starch making up about 80% of the flour's dry weight (Zobel and Kulp 1996). Food manufacturers exploit the functional properties of starches as thickening agents, gel formers, stabilizers, and in multitudes of other applications, as shown in **Table 1.1** (Satin 2000). Generally, the functional properties of a starch, as well as the degradation of those properties, are governed by the starch's amylose and amylopectin content (Johnson et al 1999; Satin 2000). Amongst starch's most important functional properties is its ability to form gels and pastes; however, with time, a process known as retrogradation can degrade the quality of starch-containing foods, giving rise to undesirable physical and textural changes in the product.

Product or process	Examples
Canning	• body or texture agent for soups, sauces, puddings and gravies • aseptically canned products • beverages such as coffee, teas or chocolate
Cereals and snacks	• hot extruded snacks • chips, pretzels, etc. • extruded and fried foods • ready-to-eat cereals
Bakery	• pies, tarts • fillings, glazes • custards and icings • cakes, donuts, danish • icing sugar
Batters and breadings	• coated fried foods • frozen battered vegetables, fish and meat • dry mix coatings
Dressings, soups and sauces	• mayonnaise-type • pourable salad dressings (high shear) • spoonable dressings • instant dry salad dressing mixes • low-fat dressing • canned gravies and sauces • frozen gravies and sauces • soups and chowders
Cooked meat binder	• water binder for formed meat • smoked meats, low-fat meats • pet foods (dried and canned)
Frozen foods	• fruit fillings • meat pies • Oriental foods • soups, sauces • entrees • cream-based products
Flavours and beverage clouds	• vitamins, spices, clouding agents • spray dried flavours for dry beverage • mixes, bartender mixes • beverage emulsions • liquid and powdered non-dairy creamers
Confectionery	• dusting powder • licorice • jelly gums • hard gums • panned candies • confectioners sugar

Dairy products	• yoghurt • cheese and imitation cheese • chilled desserts • UHT Puddings • low-fat products
Microwavable products	• cheese sauces • entrees

Table 1.1: Examples of starch uses in various food industry products (adapted from Satin 2000)

Gelatinization is the process in which starch granules when heated and dispersed in water, swell and sometimes burst, resulting in the leaching of amylose and a loss of crystalline order in the starch, ultimately forming a gel (Keetels et al 1996; Donald 2004). Conversely, retrogradation is the ageing process that occurs in a starch gel when starch reverts "from an initially amorphous state to a more ordered or crystalline state" (Gudmundsson 1994), but experimental evidence supports the notion that "long range ordering is not regained during starch retrogradation" (Keetels et al 1996). Retrogradation causes increased textural firmness and moisture loss in starch-containing products, and these changes become progressively worse and more noticeable as the product ages (Gudmundsson 1994; Zobel and Kulp 1996). Starch's component polymers, amylose and amylopectin, are believed to have differing roles in the retrogradation process. Amylose's exact role in retrogradation is not well understood; however, amylose is speculated to be capable of acting as a nucleating agent for amylopectin, and its own ability to recrystallize appears to be concentration-dependent (Zobel and Kulp 1996). Recrystallization occurs more slowly in amylopectin than amylose, and the rate at which crystallization occurs differs depending on the botanical source of the starch (Lai et al 2000). For example, rice amylopectin demonstrates a two-stage recrystallization process not seen in amylopectins derived from other botanical

sources, and the rate of retrogradation can differ between cultivars of the same cereal (Lai et al 2000). Although chemically-modified starches address some of these issues, the textural and sensory changes caused by retrogradation represent a considerable quality concern for the food industry where normal or unprocessed starches are utilized, particularly in the baked goods sector.

Methods for Measuring Amylose-Amylopectin Ratios

Numerous procedures are available for quantifying amylose content in starch and cereal grains, wherein the most commonly used methods involve measuring the complexation of iodine with amylose. In general, methods for measuring amylose content can be broken down into two categories: techniques that approximate apparent amylose content and methods that measure absolute amylose content (Johnson et al 1999). The term "apparent" amylose is often used to describe the measurements made using less sophisticated techniques such as iodine binding procedures, because many of these methods are regarded as somewhat inaccurate for various reasons (Johnson et al 1999). Furthermore, methods measuring "apparent" amylose content are regarded as less accurate than many newer methods (Johnson et al 1999). Many variations and enhancements of McCready and Hassid's (1943) original iodine binding technique have been developed. However, these modifications have resulted in great difficulty in attaining widespread acceptance of a standard method for measuring amylose. A recent study provided 17 samples of rice flour to each of 27 different labs located around the world, and tasked the researchers with determining the amylose content of the samples (Fitzgerald et al 2009). Five different variations of the colorimetric iodine binding

procedure were utilized, resulting in low reproducibility between the various labs (Fitzgerald et al 2009). The lack of a broadly adopted standard method for measuring amylose has encouraged research efforts to explore alternatives to the traditional iodine binding technique.

Iodine binding techniques are rooted in the fact that amylose generally has a stronger affinity for complexation with iodine than amylopectin, giving rise to different colorations in solution (Wang et al 1998). As such, colorimetry is a simple way for measuring the binding action of iodine with amylose; however, because iodine binding to starch's components is chain-length dependent, amylopectin can sometimes also complex with iodine, introducing inaccuracy into the method (Wang et al 1998; Bertoft 2004; Zhu et al 2008). Techniques utilizing amperometry and potentiometry have also been developed, but these analyses take longer to complete (Bates et al 1943; Larson et al 1953; Zhu et al 2008). All of the aforementioned methods involve the generation of a standard curve based on measurements of pure amylose (Zhu et al 2008). Megazyme International's amylose/amylopectin assay kit eliminates some of the inaccuracy associated with iodine binding techniques by specific precipitation of amylopectin via complexation with concanavalin A (Megazyme International Ireland 2011). This kit has seen increased use for a number of reasons: Megazyme International Ireland states that the method "is applicable to all pure starch samples and to cereal flours," analyses can be carried out without the need to generate a standard curve, and the method can be used for simultaneous determination of total starch content (Zhu et al 2008; Megazyme International Ireland 2011). But, due to the complexity and length of this approach, some

training may be required to obtain reproducible results (Zhu et al 2008). A thermogravimetric method (Stawski 2008) for determining amylose content has been developed, which also requires generation of a standard curve using pure amylose. This procedure was demonstrated to have comparable accuracy to other commonly used methods for potato and rice starches, but was incapable of reproducibly measuring amylose content of wheat starch (Stawski 2008). High performance size-exclusion chromatography has been demonstrated as being an effective tool for measuring amylose content (Grant et al 2002; Chen and Bergman 2007). Still, while these chromatographic methods offer high precision, they have relatively low throughput compared to the previously described methods (Grant et al 2002). Zhu et al (2008) conducted an extensive study comparing several of the methods already mentioned for quantifying amylose content in addition to developing a new dual-wavelength iodine binding procedure. By adding a measurement at a second wavelength to the typical colorimetric iodine binding procedure, the new method was demonstrated to have greater precision and accuracy than a single wavelength method (Zhu et al 2008). Zhu et al (2008) noted that this method still suffers from the drawbacks of a majority of other amylose determination methods: analysis times are fairly long, and the procedure lacks simplicity. Other multi-wavelength iodine binding colorimetric methods exist, like Wang's triple-wavelength method and Jarvis and Walker's sextuple-wavelength method, which are capable of providing additional information such as total starch content; however, the data analysis and procedures become more complex with the addition of more measurement wavelengths (Jarvis and Walker 1993; Wang et al 2010). However, Raman

spectroscopy combined with multivariate regression techniques may be able to overcome some of the shortfalls of other amylose determination methods.

Overview of Vibrational and Raman Spectroscopy

Vibrational spectroscopy involves the use of an assortment of instruments that impinge light on a material that then absorbs and scatters the light, in hopes of studying the vibrational and rotational actions of the substance's molecules (Kizil and Irudayaraj 2008). Raman spectroscopy, a type of vibrational spectroscopy, focuses on the detection of inelastically scattered light by Raman-active compounds. Complementary in nature to infrared spectroscopy, Raman spectroscopy can be used to observe vibrational modes that are typically of weak intensity in the IR spectrum; meanwhile, Raman spectroscopy has a weak signal for some vibrational modes that are more easily observable using IR spectroscopy. In particular, Raman spectroscopy has been demonstrated to be effective in the characterization of compounds with the following chemical characteristics: a ring structure, nonpolar character, and double or triple bonds (Kizil and Irudayaraj 2008). Extensive research efforts have been devoted to studying the industrial value and implementation of infrared and Raman spectroscopies as tools for food analysis. While infrared spectroscopy has been effectively adapted to industry use, Raman spectroscopy has never seen widespread use. Until the introduction of near-infrared excitation in the mid-1980s, Raman spectroscopy was viewed as something of an exotic technique that was unsuitable for food analysis, because food products are rarely free of impurities (Keller et al 1993). As such, instruments that used visible light excitation would be prone to introduce interference in Raman spectra in the form of fluorescence, limiting the

technique's appeal (Keller et al 1993). As an analytical tool, Raman spectroscopy offers the food industry several benefits over wet chemical techniques. The method is capable of both rapid and nondestructive testing, requires little or no sample pretreatment, and provides a tremendous amount of information about samples, which allows for the development of full-spectrum calibrations (Kizil and Irudayaraj 2008; Viereck et al 2009). Additionally, the tool has a great deal of portability, and the device's output could be coupled with infrared spectroscopy for further analysis, due to the ability of the two techniques to provide complementary information for the same sample (Viereck et al 2009). Due to the ubiquitous nature of water in food products, industry usage of mid-infrared and near-infrared spectroscopy for quantitative analysis often necessitates the employment of intricate chemometric procedures, because water absorbs strongly in the wavelength region used by these instruments (Viereck et al 2009). However, water has an inherently weak Raman signal, making the technique ideally suited for some areas of the food industry (Viereck et al 2009). Notable disadvantages of Raman spectroscopy include: considerable difficulty in producing a signal that is distinguishable from noise, and difficulty in analyzing fluorescent materials due to interferences (Viereck et al 2009). However, the advent of near-infrared laser excitation has nearly eliminated the worry of fluorescence interference with the Raman effect (Keller et al 1993). Additionally, a Raman spectroscopic method is only as accurate and precise as the wet chemical or instrumental method from which the calibration is developed, and tasks like optimization of the spectroscopic method and performance of regular instrument maintenance are necessary to maintain the multivariate calibration (Scotter 2001). Some past research has

offered hope in implementing Raman spectroscopy as an analytical tool for quality analysis of starches.

Raman Spectrum of Starch and Band Assignments

Past research has shown that most starches have a feature-rich Raman spectrum. Sample spectra of corn starch and cassava starch are shown in **Figure 1.3** (Almeida et al 2010). Researchers have elucidated many of the vibrational modes responsible for the Raman bands seen in starches. **Table 1.2** summarizes many of the spectral features shown in **Figure 1.3** (Almeida et al 2010). These band assignments can provide researchers with a basis for explaining the spectral changes that occur as a result of the physical or chemical changes being studied in an experiment.

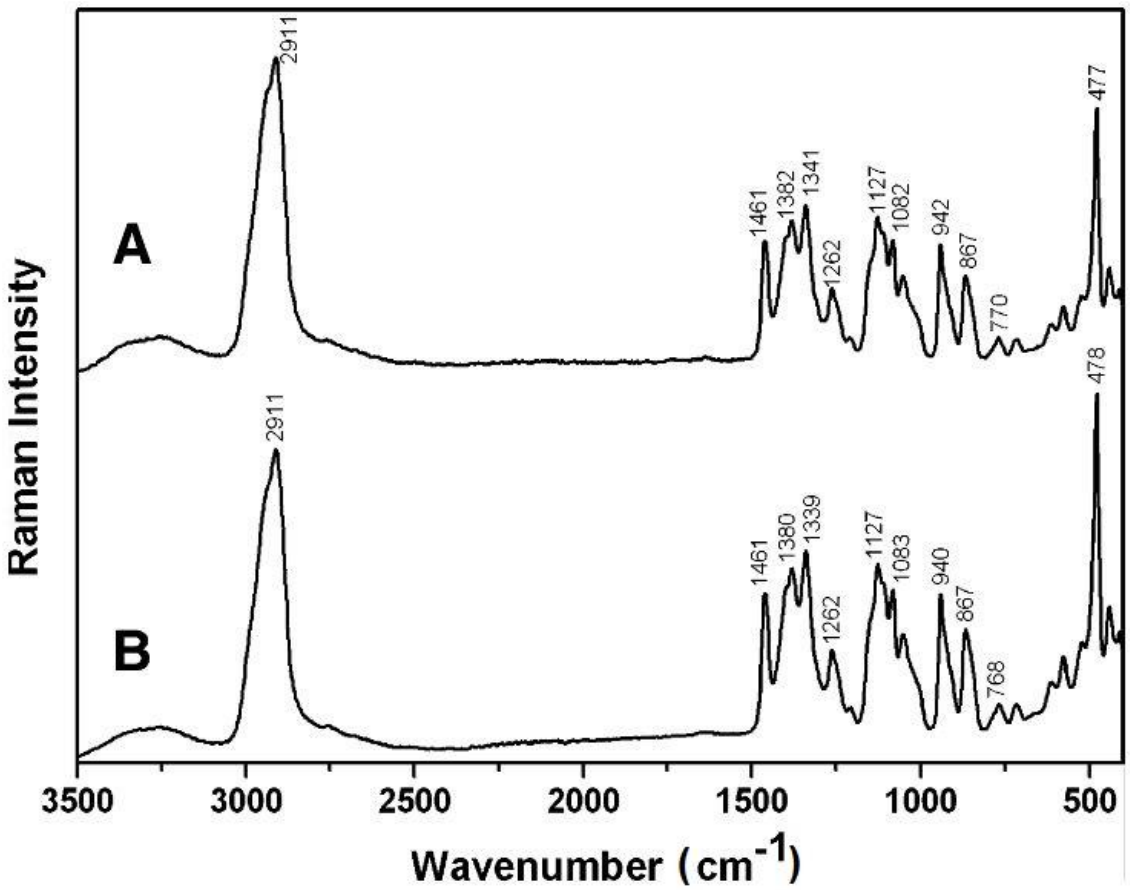

Figure 1.3: Example FT-Raman spectra of corn starch (A) and cassava starch (B) collected using 1064 nm excitation (adapted from Almeida et al 2010).

Wavenumber (cm_{-1})	Assignment	Relative Intensity
2911	C-H stretching	very strong
1461	CH, CH_2, C-O-H bending	strong
1396	C-C-H bending	strong
1380	C-O-H bending	strong
1340	C-O stretching; C-O-H bending	strong
1263	C-C-H, O-C-H, C-O-H bending	medium
1207	C-C, C-O stretching	weak
1127	C-O, C-C stretching; C-O-H bending	strong
1109	C-C, C-O stretching; C-O-H bending	strong
1083	C-O, C-C stretching; C-O-H bending	strong
1053	C-O, C-C stretching; C-O-H bending	strong
941	C-O-C, C-O-H bending; C-O stretching	strong
868	C-C-H, C-O-C bending	strong
769	C-C-O bending	weak
718	C-C-O bending	weak
615	C-C-O bending	weak
577	C-C-O bending; C-O torsion	weak
524	C-C-O bending; C-O torsion	weak
478	C-C-C bending; C-O torsion	very strong
441	C-C-O, C-C-C bending	weak
410	C-C-O, C-C-C bending	weak

Table 1.2: Raman bands seen in starch and their vibrational mode assignments as reported in the literature (table adapted from Almeida et al 2010).

Use of Raman Spectroscopy to Measure Amylose-Amylopectin Ratios

The use of Raman spectroscopy to quantify amylose content in starches has not been well researched. In particular, past research has not demonstrated whether dispersive Raman spectroscopic instruments are capable of accurately measuring amylose content in starch. Each of the following studies utilized 1064-nm excitation lasers as part of an FT-Raman spectrometer to collect the spectral data, and the most commonly used detector in these studies was a germanium detector cooled using liquid nitrogen (Phillips et al 1999; Barton et al 2000; Himmelsbach et al 2001; Sohn et al 2004; Almeida et al 2010). Phillips et al (1999) presented a Raman spectroscopic method for quantifying amylose content in corn starches. This method correlated the amylose content determined by Megazyme's amylose-amylopectin kit with the Raman spectra obtained using a FT-Raman spectrometer. Unlike many Raman and near-infrared spectroscopic methods, a simple linear regression was prepared to model the data, plotting the ratio of the integrated areas of two spectral regions of interest against measured amylose content (Phillips et al 1999). Although the method proved successful, reporting a high coefficient of determination ($r^2 = 0.997$) for the linear relationship between the bands studied and the measured amylose content, the study's scope was very limited, using only 4 total samples to demonstrate the relationship, serving as little more than a proof-of-concept (Phillips et al 1999). Barton et al (2000) developed an FT-Raman method for measuring several quality characteristics of milled rice including amylose content, which was measured using a single wavelength iodine binding colorimetric assay. The use of a multivariate calibration developed using partial least squares regression demonstrated the potential for

full-spectrum calibrations based on Raman spectral data (Barton et al 2000). An extensive follow-up study was conducted to develop an FT-Raman method for measuring amylose content of milled rice flours, this time using an autoanalyzer to perform the colorimetric iodine binding analyses (Himmelsbach et al 2001). The method was shown to be highly capable of predicting apparent amylose content of milled rice flour (8-factor PLS model, $r^2 = 0.985$, SEP = 1.05%) and reported that Raman spectroscopy could be better suited for this type of analysis than near-infrared reflectance spectroscopy, given that the proper data preprocessing steps were taken (Himmelsbach et al 2001). Raman spectroscopic methods have the potential to offer a nondestructive and rapid alternative to traditional chemical and instrumental techniques for measuring amylose content, while offering the additional benefit of being less impactful on the environment (Himmelsbach et al 2001). In another study, Sohn et al (2004) compared the abilities of NIR and FT-Raman spectroscopy to measure protein and amylose content of samples of rice flour from different crop years. Using colorimetry to generate the reference data, the researchers demonstrated that FT-Raman spectroscopy could be used to produce very reliable models (7-factor PLS model, $r^2 = 0.991$, SECV = 0.70%) for measuring amylose content (Sohn et al 2004). Additionally, FT-Raman spectroscopy was reported as being capable of producing better performing models than NIR spectroscopy, requiring fewer factors to model the data, and yielding a comparable standard error of cross-validation. Sohn et al (2004) attributed the “high precision of the models" to the use of sophisticated data preprocessing techniques, particularly orthogonal signal correction. Most recently, Almeida et al (2010) detailed a FT-Raman spectroscopic procedure for measuring the

amylose content of native corn and cassava starches, using a single-wavelength colorimetric iodine binding technique to generate reference amylose data. The researchers concluded that Raman spectroscopy could be successfully applied to the measurement of amylose content in native starches (Almeida et al 2010). However, for the corn starch model, this study used only 15 samples for the training set and 8 samples for the validation set, limiting the study's value for industrial application, where using a large number of samples (> 50) for the training set would be advisable (Almeida et al 2010).

Methods for Measuring Retrogradation in Starch

Numerous methods are available for studying retrogradation of starch and starch-containing products. Retrogradation can be monitored using a number of techniques which can be broken down into two categories: macroscopic and molecular techniques (Karim et al 2000). Macroscopic methods, chiefly rheological tests, detect physical changes that occur in a product or gel as a result of retrogradation, such as changes in viscosity. Molecular techniques aim to study molecular changes such as shifts in crystallinity (Karim et al 2000). Included in the category of macroscopic methods is instrumental texture analysis (Karim et al 2000). Though texture analysis methods encompass a variety of instruments, generally speaking, they provide researchers with quantitative information about a sample by compressing the sample in a uniform manner (Karim et al 2000). The force applied to compress the sample and the distance by which the sample was compressed can be recorded to give quantitative information about sensory attributes, like firmness, that are otherwise difficult to quantify (Karim et al

2000). Due to the sensory changes associated with the retrogradation of starch, texture analysis has been applied to study the phenomenon, particularly as a reference method for spectroscopic techniques (Xie et al 2003; Piccinini et al 2012). In industry, sensory testing remains an important tool in determining if a product is unsuitable for market; however, other macroscopic techniques such as thermal analysis have their own appeal to food manufacturers, as well.

Generally speaking, thermal analysis to monitor starch retrogradation primarily encompasses two techniques that are most widely used: differential thermal analysis (DTA) and differential scanning calorimetry (DSC) (Karim et al 2000). Using DTA, investigators can subject a starch sample and a reference material to identical thermal treatments and record the temperature difference between the two materials over a time or temperature profile, providing a means for better understanding the "physical and chemical transformations" of interest (Morita 1956; Tian et al 2011). Morita (1956) conducted one of the earliest experiments using DTA to investigate the properties of starch; however, DTA has been used somewhat sparingly in regards to specifically studying the retrogradation of starch (Karim et al 2000; Tian et al 2011). Recently, Tian et al (2011) demonstrated that DTA could be used to monitor retrogradation in rice starch gels, concluding that the coupling of DTA with differential scanning calorimetry (DSC) could give investigators a more complete understanding of starch retrogradation in cereals than either technique alone. DSC differs from DTA in a few ways in spite of the fact that similar information can be obtained using either technique. For example, equipped with a single heat source, DTA instruments allow for research applications that

may require extreme or a broad range of temperature treatments to observe and can reliably be used to ascertain transition temperature and indirect determination of enthalpies of transition for a physical or chemical phenomena of interest (Schenz 2003). Conversely, DSC, equipped with an individual heat source for the reference and sample cells, is better suited for operation at more evenly controlled heating rates and enables both the temperature and enthalpy of transition of a particular physical or chemical change to "be directly measured" (Schenz 2003). Due to its efficiency and simplicity, DSC remains a popular tool for quantifying retrogradation by the detection of melting endotherms (Karim et al 2000). Researchers can use DSC to obtain detailed information about phase transitions in foods, such as the melting of amylopectin and its associated enthalpy (Karim et al 2000). The ease of the generalized DSC procedure for monitoring retrogradation may make it appealing to food manufacturers (Karim et al 2000). Additionally, DSC can be used to measure retrogradation in multiple food matrices such as bread and waxy starch gels, to name a few (Ribotta et al 2004; Liu et al 2010; Tian et al 2011). Karim et al (2000) noted that studying starch gels with DSC require a commonly reported minimum starch concentration of 20%. Though macroscopic techniques are normally more accessible to food manufacturers, molecular techniques such as X-ray diffraction have remained a staple of academic research for many decades.

X-ray diffraction has offered academia a potent tool for elucidating molecular structures of crystalline or semi-crystalline materials; however, its use as an analytical tool in the food industry is likely limited somewhat due to the expense associated with the instrumentation. Nevertheless, research has developed methods for measuring the

relative percentages of the crystalline and amorphous phases in starches (Nara et al 1978), allowing investigators to study retrogradation at the molecular level, and providing researchers with information on specific phenomena relating to retrogradation like the staling of bread (Karim et al 2000; Ribotta et al 2004). Such experiments have been conducted on starch, starch gels and solutions, and recently on model food products like baked bread (Karim et al 2000; Ribotta et al 2004). However, the method may have disadvantages when compared to some other available procedures. Kim et al (1997) performed a study comparing three different methods for measuring the "degree of retrogradation" in rice starch gels: DSC, X-ray diffraction and the α-amylase-iodine method. Kim et al (1997) remarked that X-ray diffraction was the least sensitive of the three methods. This sentiment was echoed by Karim et al (2000), who noted that past experimental evidence indicated that spectroscopic techniques like FT-infrared and nuclear magnetic resonance spectroscopy had the potential to be more sensitive.

Another broad group of molecular techniques are spectroscopic methods, which include a variety of procedures and instruments that can be used to study starch retrogradation. Several spectroscopic techniques have been developed for studying the chemical process and kinetics of retrogradation using Raman spectroscopy (Bulkin et al 1987), FT-infrared spectroscopy (Goodfellow and Wilson 1990) and nuclear magnetic resonance spectroscopy (Yao and Ding 2002).

Some of the aforementioned methods, with the exception of thermal analysis, texture analysis and sensory testing, are economically impractical for industry application or have not been demonstrated as having such applicability. Although its applications

have only begun to be researched, Raman spectroscopy remains a possibility for monitoring starch retrogradation in industry.

Use of Raman Spectroscopy to Measure Retrogradation

Some of the earliest work using Raman spectroscopy to monitor retrogradation of starch was performed by Bulkin et al (1987). By monitoring changes in the full width half-height (FWHH) of a band around 480 cm^{-1}, and another in the region of 2800 cm^{-1} to 3000 cm^{-1}, Bulkin et al (1987) demonstrated that molecular changes could be monitored in a waxy corn starch/water slurry over a 20-hour period using rapid Raman scanning. Going further, the band around 480 cm^{-1} was shown as being effective at observing spectral changes relating to retrogradation over a time period of two weeks (Bulkin et al 1987). These data were used to put forward a 4-step mechanism by which retrogradation occurred in the observed starch gels, and by which small angle X-ray scattering and wide angle X-ray diffraction were used to support the proposed kinetics of the mechanism (Bulkin et al 1987). Utilizing the findings of Bulkin et al (1987) and applying them to the study of starches from other botanical sources, Fechner et al (2005) explored the utility of monitoring the FWHHs as well as shifts in the wavenumber position of the Raman bands identified in Bulkin's study, demonstrating that a very small but measurable change was occurring in many of the of the starches studied. Neither study attempted to statistically correlate their findings with an existing method for measuring starch retrogradation. Kim et al (1989) performed a study using Raman spectroscopy with visible light excitation to monitor the gelatinization of waxy corn starch. Kim et al (1989) compared the Raman spectra of raw starch and starch that had just been gelatinized, noting major changes in

the intensity and position of many bands. Kim et al (1989) noted that the band at 475 to 480 cm^{-1} exhibited a shift from being of very strong intensity before gelatinization to being very weak immediately after. Additionally, the researchers noted that most Raman bands exhibited a decreased intensity immediately following gelatinization, while some bands also shifted from their original position in the spectrum of raw starch, with some bands shifting by 10 cm^{-1} or more (Kim et al 1989). The researchers proposed a model for what was happening at the molecular level and suggested using a ratio of wavenumbers as "indices of the degree of gelatinization" (Kim et al 1989). Since the researchers were only interested in studying gelatinization kinetics, the experiment was not extended further to look at the potential of monitoring retrogradation; however, their research gives insight into what the immediate impact of gelatinization might be on the Raman spectra of starch gels (Kim et al 1989). Piccinini et al (2012) explored the application of FT-Raman spectroscopy to the monitoring of starch retrogradation in semolina bread. The researchers prepared loaves of bread using semolina flour and stored them under controlled conditions, collecting both Raman spectra and firmness measurements from a texture analyzer at selected intervals over a period of 20 days (Piccinini et al 2012). Synchronous 2-D correlation analysis was applied to determine which bands in selected regions of interest underwent the most significant changes during the course of the experiment (Piccinini et al 2012). Supported by past evidence, but also noting that other spectral regions exhibited changes, the researchers chose to focus primarily on the Raman band at 480 cm^{-1} (Piccinini et al 2012). Piccinini et al (2012) reported a strong correlation between bread firmness measurements and the change in the

FWHH of the 480 cm^{-1} band (Piccinini et al 2012). Piccinini et al (2012) also noted that the frequency of the 480 cm^{-1} band shifted roughly 1 cm^{-1} while the FWWH of the band at 480 cm^{-1} also decreased by less than 1 cm^{-1} over the 20-day duration of the experiment. Of additional note, the researchers reported that over the course of the study a band appeared at about 765 cm^{-1} that would merit additional study (Piccinini et al 2012). Flores-Morales et al (2012) performed another study using Raman spectroscopy to look at the chemical changes that occur as a result of nixtamalization and the retrogradation of starch isolated from both freshly-baked tortillas and tortillas that had been stored for 10 days at refrigeration temperatures. However, as with several of the previously mentioned studies, the researchers did not attempt to correlate their findings with any other existing methods for studying starch retrogradation, choosing instead to comment on relative changes in the spectra before and after storage (Flores-Morales et al 2012). Flores-Morales et al (2012) noted that the bands at 480 and 2900 cm^{-1} appeared to show changes as a result of retrogradation. Additionally, bands at 856, 1127 and 1459 cm^{-1} were reported to show a general decrease in intensity as a result of the process (Flores-Morales et al 2012). Outside of these studies, little work has been performed using Raman spectroscopy to monitor retrogradation in starch gels and in food models. Of ancillary importance due to the complementary nature of infrared spectroscopy, Xie et al (2003) demonstrated that near-infrared reflectance spectroscopy could more effectively measure staling in white pan breads than texture analysis could. The spectroscopic technique was shown to have a high correlation with firmness values measured by texture analysis (Xie et al 2003). Ultimately, the method was demonstrated as being more exact at measuring

bread storage time than texture analysis, because the near-infrared method was able to monitor more of the changes that occured during staling such as moisture loss (Xie et al 2003). The work done by Xie et al (2003) highlights a potential but likely insignificant drawback to using Raman spectroscopy: Raman spectroscopy traditionally has a very weak signal for water.

References

Almeida, M. R., Alves, R. S., Nascimbem, L. B. L. R., Stephani, R., Poppi, R. J., and de Oliveira, L. F. C. 2010. Determination of amylose content in starch using Raman spectroscopy and multivariate calibration analysis. Anal. Bioanal. Chem. 397:2693-2701.

Barton, F. E., Himmelsbach, D. S., McClung, A. M., and Champagne, E. T. 2000. Rice quality by spectroscopic analysis: precision of three spectral regions. Cereal Chem. 77:669-672.

Bates, F. L, French, D., and Rundel, R. E. 1943. Amylose and amylopectin content of starches determined by their iodine complex formation. J. Am. Chem. Soc. 65: 142-148.

Bertoft, E. 2004. Analysing Starch Structure. Pages 57-96 in: Starch in food: Structure, function and applications. A.-C. Eliasson, ed. CRC Press: Boca Raton.

Bulkin, B. J., Kwak, Y., and Dea, I. C. M. 1987. Retrogradation kinetics of waxy-corn and potato starches; a rapid, Raman-spectroscopic study. Carbohydr. Res. 160:95-112.

Chen, M.-H., and Bergman, C. J. 2007. Method for determining the amylose content, molecular weights, and weight- and molar-based distributions of degree of polymerization of amylose and fine-structure of amylopectin. Carbohydr. Polym. 69:562-578.

Chinnaswamy, R., and Hanna, M. A. 1988. Relationship between amylose content and extrusion-expansion properties of corn starches. Cereal Chem. 65:138-143.

Donald, A. M. Understanding Starch Structure and Functionality. Pages 156-184 in: Starch in food: Structure, function and applications. A-C. Eliasson, ed. CRC Press: Boca Raton.

Fechner, P. M., Wartewig, S., Kleinebudde, P., and Neubert, R. H. H. 2005. Studies of the retrogradation process for various starch gels using Raman spectroscopy. Carbohydr. Res. 340:2563-2568.

Fitzgerald, M. A., Bergman, C. J., Ressurreccion, A. P., Moller, J., Jimenez, R., Reinke, R. F., Martin, M., Blanco, P., Molina, F., Chen, M., Kuri, V., Romero, M. V., Habibi, F., Umemoto, T., Jongdee, S., Graterol, E., Reddy, K. R., Bassinello, P. Z., Sivakami, R., Rani, N. S., Das, S., Wang, Y., Indrasari, S. D., Ramli, A., Ahmad, R., Dipti, S. S., Xie, L., Lang, N. T., Singh, P., Toro, D. C., Tavasoli, F. and Mestres C. 2009. Addressing the dilemmas of measuring amylose in rice. Cereal Chem. 86:492-498.

Flores-Morales, A., Jiménez-Estrada, M., and Mora-Escobedo, R. 2012. Determination of the structural changes by FT-IR, Raman, and CP/MAS ^{13}C NMR spectroscopy on retrograded starch of maize tortillas. Carbohydr. Polym. 87:61-68.

Goodfellow, B. J., and Wilson, R. H. 1990. A Fourier transform IR study of the gelation of amylose and amylopectin. Biopolymers 30:1183-1189.

Grant, L. A., Ostenson, A. M., and Rayas-Duarte, P. 2002. Determination of amylose and amylopectin of wheat starch using high performance size-exclusion chromatography. Cereal Chem. 79:771-773.

Gudmundsson, M. 1994. Retrogradation of starch and the role of its components. Thermochim. Acta 246:329-341.

Himmelsbach, D. S., Barton, F. E., McClung, M. A., and Champagne, E. T. 2001. Protein and apparent amylose contents of milled rice by NIR-FT/Raman spectroscopy. Cereal Chem. 78:488-492.

Hoseney, C. R. 1998. Starch. Pages 29-64 in: Principles of Cereal Science and Technology. American Association of Cereal Chemists, Inc.: St. Paul.

Jane, J., Chen, Y. Y., Lee, L. F., McPherson, A. E., Wong, K. S., Radosavljevic, M., and Kasemsuwan, T. 1999. Effects of amylopectin branch chain length and amylose content on the gelatinization and pasting properties of starch. Cereal Chem. 76:629-637.

Jarvis, C. E., and Walker, J. R. L. 1993. Simultaneous, rapid, spectrophotometric determination of total starch, amylose and amylopectin. J. Sci. Food Agric. 63:53-57.

Johnson, L. A., Baumel, C. P., Hardy, C. L., and White, P. J. 1999. Identifying Valuable Corn Quality Traits for Starch Production. Iowa State University Extension: Ames. Available online at: http://www.extension.iastate.edu/Publications/EDC194.pdf.

Karim, A. A., Norziah, M. H., and Seow, C. C. 2000. Methods for the study of starch retrogradation. Food Chem. 71:9-36.

Keetels, C. J. A. M., Oostergetel, G. T., and van Vliet, T. 1996. Recrystallization of amylopectin in concentrated starch gels. Carbohydr. Polym. 30: 61-64.

Keller, S., Löchte, T., Dippel, B., and Schrader, B. 1993. Quality control of food with near-infrared-excited Raman spectroscopy. Fresenius' J. Anal. Chem. 346:863-867.

Kim, I.-H., Yeh, A., Zhao, B. L., and Wang, S. S. 1989. Gelatinization kinetics of starch by using Raman spectroscopy. Biotechnol. Prog. 5:172-174.

Kim, J.-O., Kim, W.-S., and Shin, M.-S. 1997. A comparative study on retrogradation of rice starch gels by DSC, X-ray and alpha-amylase methods. Starch/Starke 49:71-75.

Kizil, R., and Irudayaraj, J. 2008. Applications of Raman Spectroscopy for Food Quality Measurement. Pages 143-163 in: Nondestructive Testing of Food Quality. J. Irudayaraj and C. Reh, eds. Blackwell Publishing: Ames.

Lai, V. M-.F., Lu, S., and Lii, C.-Y. 2000. Molecular characteristics influencing retrogradation of rice amylopectins. Cereal Chem. 77:272-278.

Larson, B. L., Gilles, K. A., and Jenness, R. 1953. Amperometric method for determining the sorption of iodine by starch. Anal. Chem. 25:802-804.

Lee, M.-R., Swanson, B. G., and Baik, B.-K. 2001. Influence of amylose content on properties of wheat starch and breadmaking quality of starch and gluten blends. Cereal Chem. 78:701-706.

Liu, H., Yu, L., Tong, Z., and Chen, L. 2010. Retrogradation of waxy cornstarch studied by DSC. Starch/Starke 62:524-529.

McCready, R. M., and Hassid, W. Z. 1943. The separation and quantitative estimation of amylose and amylopectin in potato starch. J. Am. Chem. Soc. 65:1154-1157.

Megazyme International Ireland. 2011. Amylose/amylopectin assay procedure for the measurement of the amylose and amylopectin contents of starch. Megazyme International Ireland: Bray. Available online at: http://www.megazyme.com/downloads/en/data/K-AMYL.pdf

Morita, H. 1956. Characterization of starch and related polysaccharides by differential thermal analysis. Anal. Chem. 28:64-67.

National Center for Biotechnology Information. 2005. Image of the 2-D structure of amylopectin. National Center for Biotechnology Information: Bethesda. Available online at: http://pubchem.ncbi.nlm.nih.gov/summary/summary.cgi?cid=439207&loc=ec_rcs#x281

National Center for Biotechnology Information. 2011. Image of the 2-D structure of amylose. National Center for Biotechnology Information: Bethesda. Available online at: http://pubchem.ncbi.nlm.nih.gov/summary/summary.cgi?cid=53477771&loc=ec_rcs

Nara, S., Mori, A., and Komiya, T. 1978. Study on relative crystallinity of moist potato starch. Starch/Starke 30:111-114.

Phillips, D. L., Xing, J., Liu, H., Pan, D.-H., and Corke, H. 1999. Potential use of Raman spectroscopy for determination of amylose content in maize starch. Cereal Chem. 76:821-823.

Piccinini, M., Simonetta, F., Secchi, N., Sanna, M., Roggio, T., and Catzeddu, P. 2012. The application of NIR FT-Raman spectroscopy to monitor starch retrogradation and crumb firmness in semolina bread. Available online only. doi: 10.1007/s12161-011-9360-8. Springer-Verlag, Berlin, Germany.

Ribotta, P. D., Cuffini, S., León, A. E., and Añón, M. C. 2004. The staling of bread: an X-ray diffraction study. Eur. Food. Res. Technol. 218:219-223.

Satin, M. 2000. Functional Properties of Starches. FAO Agriculture and Consumer Protection Department: Rome. Available online at: http://www.fao.org/ag/magazine/pdf/starches.pdf

Schenz, T. 2003. Thermal Analysis. Pages 517-528 in: Food Analysis. S. S. Nielsen, ed. Springer Science+Business Media LLC: New York.

Scotter, C. N. G. 2001. NIR Techniques in Cereals Analysis. Pages 90-99 in: Cereals and Cereal Products: Chemistry and Technology. D. A. V. Dendy and B. J. Dobraszczyk, eds. Aspen Publishing: Gaithersburg.

Sohn, M., Himmelsbach, D. S., and Barton, F. E. 2004. A comparative study of Fourier transform Raman and NIR spectroscopic methods for assessment of protein and apparent amylose in rice. Cereal Chem. 81: 429-433.

Stawski, D. 2008. New determination method of amylose content in potato starch. Food Chem. 110:777-781.

Tian, Y., Xu, X., Xie, Z., Zhao, J., and Jin, Z. 2011. Starch retrogradation determined by differential thermal analysis (DTA). Food Hydrocolloids 25:1637-1639.

USDA Economic Research Service. 2011. Feed Grains Data Yearbook Tables – Corn: Food, seed, and industrial use. USDA: Washington. Available online at: http://www.ers.usda.gov/Data/FeedGrains/Table.asp?t=31.

Viereck, N., Salomonsen, T., van den Berg, F., and Engelsen, S. B. 2009. Raman Applications in Food Analysis. Pages 199-223 in: Raman Spectroscopy for Soft Matter Applications. M. S. Amer, ed. John Wiley & Sons: Hoboken.

Wang, J. P., Li, Y., Tian, Y. Q., Xu, X. M., Ji, X. X., Cao, X., and Jin, Z. Y. 2010. A novel triple-wavelength colorimetric method for measuring amylose and amylopectin contents. Starch/Starke 62:508-516.

Wang, T. L., Bogracheva, T. Y., and Hedley, C. L. 1998. Starch: as simple as A, B, C?. J. Exp. Bot. 49:481-502.

Xie, F., Dowell, F. E., and Sun, X. S. 2003. Comparison of near-infrared reflectance spectroscopy and texture analyzer for measuring wheat bread changes in storage. Cereal Chem. 80:25-29.

Yao, Y., and Ding, X. 2002. Pulsed nuclear magnetic resonance study of rice starch retrogradation. Cereal Chem. 79:751-756.

Zhu, T., Jackson, D. S., Wehling, R. L., and Geera, B. 2008. Comparison of amylose determination methods and the development of a dual wavelength iodine binding technique. Cereal Chem. 85:51-58.

Zobel, H. F., and Kulp, K. 1996. The Staling Mechanism. Pages 1-64 in: Baked Goods Freshness: Technology, Evaluation, and Inhibition of Staling. R. E. Hebeda and H. F. Zobel, eds. Marcel Dekker: New York.

CHAPTER II: DEVELOPMENT OF A RAMAN SPECTROSCOPIC METHOD FOR MEASURING AMYLOSE-AMYLOPECTIN RATIOS OF CORN STARCH

Abstract

An investigation utilizing Raman spectroscopy to measure the amylose-amylopectin ratio of corn starch was conducted. Amylose-amylopectin ratios impact quality and functional properties of starch and starch-containing food systems. However, the food industry lacks rapid non-destructive methods for measuring these quality parameters. Raman spectroscopy may be able to offer a rapid alternative to traditional wet-chemical methods. Sixty-seven samples of corn starch ranging from -1.4% to 23.2% amylose were prepared by randomly mixing selected starches from 2 sources of normal starch and 3 sources of waxy (high amylopectin) starch. Samples were placed in 1.8-ml glass vials and sealed with screw caps prior to being measured. Raman spectra were collected over the region of 250 cm^{-1} to 3200 cm^{-1} using a Raman spectrometer with an excitation wavelength of 785 nm. Scanning parameters were optimized, with a 60 second integration time and averaging of duplicate scans provided satisfactory results. Reference amylose content values for each sample were determined by colorimetry using a dual-wavelength iodine binding method. Multivariate models were prepared. Samples were subdivided into a calibration set (n=45) and a validation set (n=22). Partial least squares regression and principal component regression algorithms were used to prepare calibration models. Eliminating the spectral region above 2000 cm^{-1} improved the performance of the calibration models. PLS regression yielded the best model performance (r^2 of validation = 0.832 for a 7-factor model, SEP = 2.90%). Excluding samples made with cold water swelling starch offered minor improvement in model performance. Other preprocessing treatments and data manipulation methods including differentiation of spectra using the Savitzky-Golay method and truncation of the

calibration sample set based on reference amylose content were explored but did not yield improved results.

Introduction

Starch is a key and versatile food ingredient which can be used to serve a variety of needs in manufacturing due to its numerous functional properties. A few of these include its ability to form pastes and gels, thicken sauces as well as other mixtures and stabilize emulsions (Satin 2000). Many of the important functional properties of starch, and their impact and usage in foods, are controlled by the relative proportions of the two polymers that comprise starch, amylose and amylopectin (Johnson et al 1999; Satin 2000). As such, amylose content of starches and starch-containing products is a key quality parameter. Although various methods are available to measure amylose content, measuring this attribute rapidly can be difficult.

Two broad categories of techniques are available: those that measure "apparent amylose" and those that measure "absolute amylose" (Johnson et al 1999). The term "apparent amylose" is often used to describe the result of older techniques, because the result is called into question due to inherent inaccuracy associated with the method (Johnson et al 1999; Himmelsbach et al 2001). As an example, measuring iodine's complexation with amylose is one of the principal ways of determining "apparent amylose," encompassing several techniques such as potentiometry, amperometry and colorimetry (Bates et al 1943; Larson et al 1953; Himmelsbach et al 2001; Zhu et al 2008). However, the iodine binding capacity of amylose and amylopectin exhibits chain-length dependence, meaning that amylopectin is also capable of forming inclusion

complexes with iodine (Wang et al 1998; Bertoft 2004). Colorimetric determination procedures for amylose content may be the most commonly used techniques due to their relative ease when compared to older methods (Zhu et al 2008). Though relatively inexpensive to perform, the desirability of these methods for routine industry use or use by crop improvement initiatives may be diminished somewhat due to the fact that these techniques are destructive, complicated and are observed as not being very precise. A survey found that the imprecision of these techniques may be in part related to variations in how standard curves are generated between laboratories; furthermore, the lack of an accepted standard method for measuring amylose content could have contributed, resulting in a wide variety of procedures being used worldwide (Fitzgerald et al 2009).

Spectroscopic methods, which are capable of overcoming some of the limitations of iodine binding procedures, have been researched more intensely in recent years, with researchers contributing both near-infrared (NIR) and Fourier transform (FT) Raman spectroscopic methods to the knowledge base. FT-Raman spectroscopy has been demonstrated as a possible alternative to NIR spectroscopy for measuring amylose content of maize and cassava starches, but only in a very limited scope (Phillips et al 1999; Almeida et al 2010). FT-Raman spectroscopic techniques for measuring multiple quality attributes of milled rice and rice flour, including amylose content, have been developed with great success (Barton et al 2000; Himmelsbach et al 2001; Sohn et al 2004). In fact, when compared with NIR spectroscopy, experimental evidence supported the notion that FT-Raman spectroscopy may be superior or equally capable for quantifying amylose content when spectral data was treated with sophisticated data

preprocessing algorithms (Sohn et al 2004). Though several methods have been developed using FT-Raman spectroscopy to measure amylose content of starch and starch-based products, the authors are unaware of any methods using a relatively inexpensive and portable dispersive Raman spectroscopic instruments. Moreover, many existing methods are based on reference data collected using single wavelength iodine binding colorimetric techniques, which may be less precise and provide less information than dual-wavelength or multi-wavelength colorimetric procedures (Jarvis and Walker 1993; Zhu et al 2008; Wang et al 2010). As such, the objective of this study was to develop, optimize, validate and evaluate the efficacy of an inexpensive Raman spectroscopic method for quantifying amylose-amylopectin ratios in corn starch.

Materials & Methods

Corn starch mixture preparation

Blended samples of normal and waxy corn starches were prepared. The following corn starches were utilized for sample preparation: National Starch AMIOCA (waxy), National Starch NOVATION 4600 (waxy), National Starch NOVATION 2600 (waxy), National Starch MELOJEL (normal) and Argo Corn Starch (normal). National Starch AMIOCA (Bridgewater, NJ) and National Starch MELOJEL samples were obtained from the University of Nebraska – Lincoln's Food Processing Center. Dr. Devin Rose (UNL – Food Science & Technology Dept.) provided National Starch NOVATION 4600 and National Starch NOVATION 2600 samples. Argo Corn Starch (ACH Food Companies, Memphis, TN) was purchased from a local grocery store (HyVee). Eighty-one samples were prepared using a random design and by mixing one waxy starch with one normal

starch on the basis of waxy starch content (w/w), and their concentrations ranged from 0% to 100% waxy starch, with concentrations spaced in 5% increments. Each sample weighed 50 ± 0.02 g total. Each unique combination of the available normal and waxy starches was given a code ranging from 1-6, which was used in combination with a random number generator (RANDOM.org) to assign which normal and waxy starches were blended to prepare each sample. Using this method, a mixing protocol was prepared (**Table A-1** and **A-2** in the appendix). Samples were weighed into a weigh boat using a top-loading balance and then stirred for 1 minute with a spatula and shaken in a glass jar for 1 minute to ensure thorough mixing, and samples were then transferred to glass sample containers with screw-cap lids for storage.

Sample preparation for Raman spectroscopy

Using a spatula, starch samples were transferred to 1.8-ml short-form style glass vials with phenolic screw caps (VWR, Radnor, PA). The vials were filled no less than half full. Vials were sealed using the provided screw caps and stored in a drawer at ambient temperature until the scans were made. Vials were prepared in duplicate for each sample to account for potential spectral differences that may arise from how samples were packed or differences in the sample vials.

Raman spectroscopy

All Raman spectral data were collected using an Enwave Optronics EZRaman-M series Raman spectrometer (Irvine, CA) connected to a laptop. The EZRaman Reader software provided with the Raman analyzer was used to handle the data collection. Sample spectra were measured in the region of 250 cm^{-1} to 3200 cm^{-1} with a optical

resolution of 6 cm^{-1}. The excitation wavelength of the laser was 785 nm, while the power of the laser was set at approximately 300 to 400 mW. The EZRaman Reader software's Auto Baseline correction function was used in the collection of all spectral data. Before scanning, sample vials were cleaned with a KimWipe to remove any fingerprints or residues that may interfere with data collection. Each sample vial was measured in duplicate by rotating the vial 90° between scans.

Spectral collection optimization

To determine the optimal spectral collection parameters for use in the method, a small preliminary experiment was carried out by scanning starch samples of varying amylose contents. One normal corn starch (Penford Food Ingredients, Centennial, CO), one high amylose corn starch (Cargill, Wayzata, MN) and one waxy corn starch (Staley) were each measured using the Raman spectrometer, and the spectral collection parameters were varied to assess their impact on spectral quality. The EZRaman Reader software's "Quick Scan" function was used to establish initial scanning parameters. Afterwards, the following spectral collection parameters were varied: the integration time, the number of scans to collect and average, and the smoothing level. Each sample was scanned in triplicate, and replicate scans were achieved by rotating the sample 90° between scans. Optimal parameters were determined to be an integration time of 60 s, the collection of an average of 2 scans, and a smoothing level of 1. These parameters were used for the collection of all spectral data for the experiment.

Reference analysis

A modified version of the dual wavelength iodine binding colorimetric method described by Zhu et al (2008) was used to determine the amylose-amylopectin ratio of each sample. All reagents were prepared in the manner described by Zhu et al (2008). Each sample was prepared and measured in triplicate. Starch (100.0 ± 0.5 mg) was weighed on an as is basis using an analytical balance and transferred to a plastic 50-ml centrifuge tube. Using a micropipetter (Gilson, Middleton, WI), 1 ml of reagent alcohol was added to the tube. The tube was then vortexed at max speed for about 20 s. A volumetric pipet was used to transfer 10 ml of 1 N sodium hydroxide (NaOH) to the tube. The tube was vortexed at max speed for about 20 s, allowed to stand for about 10 s and then vortexed at max speed for another 20 s to ensure thorough mixing. Each tube was capped with the provided screw cap and allowed to sit for 1 h until the solution became clear. After the time elapsed, the solution was transferred to a 100-ml volumetric flask. The centrifuge tube was then washed with about 20 ml of distilled water and vortexed at max speed for about 20 s, and the contents were then transferred to the volumetric flask as well. This process was repeated twice for each sample. Each flask containing a sample was then diluted to volume with distilled water. Two ml of each diluted sample were then transferred to a new 100-ml volumetric flask. Approximately 50 ml of distilled water and 2 drops of phenolphthalein indicator were added to each flask. The resultant mixture was carefully titrated with 0.1 N hydrochloric acid (HCl) to a colorless endpoint. Two ml of 0.2% iodine solution were added to each flask, and each flask was then diluted to volume with distilled water. Flasks were stored in a dark cabinet for about 30 min to fully develop color. Samples were measured from 400 to 700 nm using a Beckman DU-

520 UV-Vis spectrophotometer (Beckman-Coulter, Brea, CA), and the absorbance values at 510 and 620 nm were recorded. Distilled water was used as a blank; samples were measured in glass cuvettes. Each sample was scanned in duplicate, and the absorbance readings at each wavelength were averaged. Amylose content was calculated using **Equation 2.1** described by Zhu et al (2008) for determining the amylose content of starches from cereal sources using the dual wavelength iodine binding technique.

Equation 2.1: $\%\ Amylose = \frac{(Diff\ ABS + 0.0542)}{0.3995}$,
where Diff ABS = Abs @ 620 nm – Abs @ 510 nm

Replicate reference results were averaged, and the relative standard deviation and standard deviation were used to assess the precision of the data. Reference data were accepted or rejected using one of two limitations: replicates must have a relative standard deviation (RSD) equal to or less than 5% for samples estimated to be above 5% amylose content, or samples must have an absolute standard deviation less than or equal to 0.3% amylose content for samples estimated to be at or below 5% amylose content. Reference data that did not meet the limits for precision were not included in the calibration or validation data sets. The described calculations were performed using Microsoft Excel 2007.

Data preprocessing and chemometrics

Data preprocessing of spectra was performed in GRAMS/AI 8.0 (Thermo Scientific, Woburn, MA). Specific procedures that were used for each spectral measurement are spectral linearization (XY2Even.AB) and spectral averaging of replicate spectra (Average.AB). The complementary PLSplus/IQ software module was used for

development of calibration models. For the development and validation of the calibration models, the samples were split into subsets: a training set and a validation set. The subsets were prepared by putting the samples in numerical order, and every third sample was put in the validation dataset. Furthermore, additional data preprocessing steps such as mean centering and spectral region restrictions were assessed and utilized based on their ability to improve the calibration model. Calibrations were prepared using the PLS-1 and PCR algorithms made available through the PLSplus/IQ software, and a cross-validation was performed for each model using the software's built-in leave-one-out method. Each model was prepared with mean centering, and any truncations of the spectral region of interest were set using the software. The number of factors used in a calibration model was determined by selecting the number of factors that minimizes the prediction residual error sum of squares without overfitting the data. Preparing a plot of the prediction residual error sum of squares vs. the number of factors was used to achieve that goal. Initial assessments of model performance were based on the r^2 value of the line of best fit for the instrument-predicted value vs. the experimental value of the calibration sample set, the standard error of cross-validation (SECV) and trends of overestimation or underestimation of calibration samples predicted by the model. Samples in the validation set were predicted using the PLSplus/IQ software add-on available through GRAMS/AI 8.0. The performance of each multivariate calibration was evaluated based upon assessment of the r^2 value of the line of best fit for the instrument-predicted value vs. the experimental value of an independent validation sample set, the standard error of prediction (SEP), the ratio of the standard error of prediction to the sample standard

deviation (RPD), bias and trends of overestimation or underestimation of samples predicted by the model. The equations used to calculate these measures, except RPD, were described in the PLSplus/IQ user's guide (Galactic Industries Corporation 1996). The equation used to calculate RPD is described by Williams (2004). These calculations were made using Microsoft Excel 2007.

Results & Discussion

Preliminary experiments to determine optimal scanning parameters revealed that a 60 second integration time, collecting and averaging of 2 scans per sample vial, and a smoothing level of 1 resulted in satisfactory spectra. Longer integration times did not offer a considerable improvement in the signal-to-noise ratio, and additional smoothing beyond the minimum was not deemed necessary as almost all of the typical spectral features of starch were observed clearly. Preliminary experiments were performed using an independent set of 20 samples of waxy (Staley)/normal corn starch (Penford Food Ingredients) mixtures. Samples ranged from 25 to 85% waxy starch with uneven spacing between sample increments. Calibration models prepared on the basis of measuring percent waxy corn starch showed results that were encouraging enough (r^2 of calibration $\geq .7$) to justify proceeding with the generation of an expanded sample set and collection of reference data. An example of the typical Raman spectrum of Argo normal corn starch, obtained using the optimized collection parameters, is shown in **Figure 2.1**.

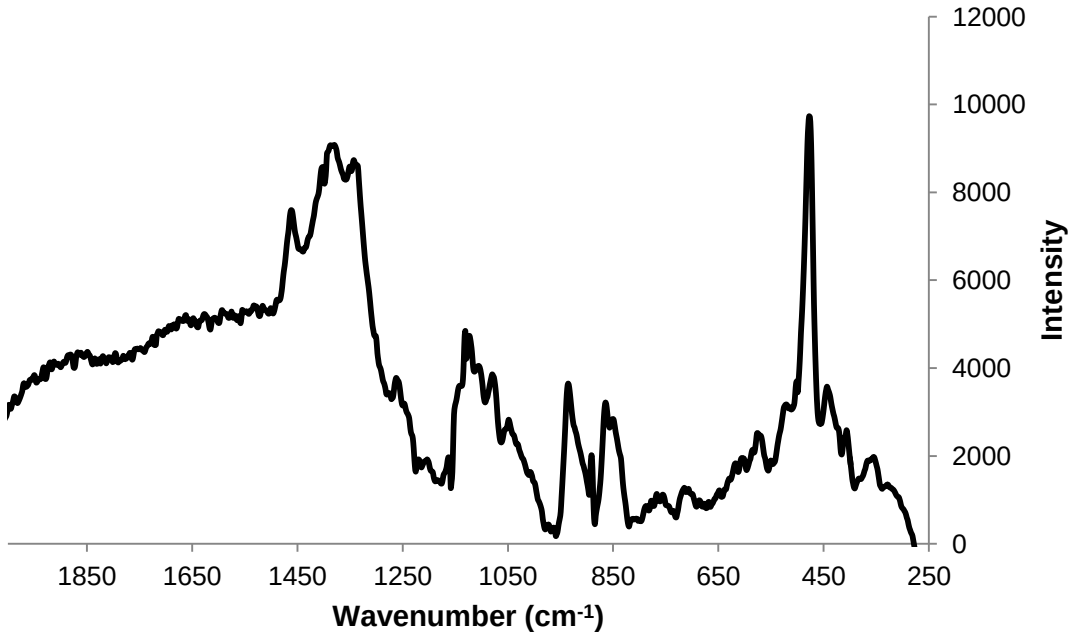

Figure 2.1: Example of the typical Raman spectrum of Argo normal corn starch collected using 785 nm (near-infrared) excitation. Spectrum has been truncated to 2000 to 250 cm^{-1}.

The majority of the Raman bands occured between 250 and 1500 cm^{-1}, which is consistent with the band information commonly reported for starch in the literature (Almeida et al 2010). A broad spectral feature appeared between 1500 cm^{-1} and 2000 cm^{-1}, but the cause is unclear and requires further study. Using 785 nm excitation, the band commonly reported to peak around 2900 to 2910 cm^{-1}, associated with CH stretching, was not easily visible and not well resolved (Almeida et al 2010). This appeared to be the only spectral band that was lost or diminished in intensity by using 785 nm excitation as opposed to 1064 nm excitation. As such, although full region models were prepared, the region between 250 and 2000 cm^{-1} became the primary focus of the study. Poor sampling has been identified as a concern when using Raman spectroscopy to measure amylose content of milled rice; use of a spinning cup apparatus

was suggested as a means to overcome this problem (Himmelsbach et al 2001). Due to the small particle size of starch, this should be less of an issue; however, the instrument used in this experiment did not allow for simple implementation of such a solution, so samples were rotated manually approximately 90° between replicate scans to improve the sampling of each vial. Examining the spectra of both waxy and normal starch samples affirmed the findings of previous researchers: differences in the spectral features of amylose and amylopectin are minor and not easily discerned visually (Himmelsbach et al 2001). Thus, multivariate statistical methods were employed to measure any spectral variation between samples, because analysis of multiple bands has been shown to be effective in quantifying amylose content of starches and starch-containing products (Barton et al 2000; Himmelsbach et al 2001; Sohn et al 2004; Almeida et al 2010).

The amylose content of each starch mixture was determined using a modified version of Zhu's (2008) dual wavelength colorimetric iodine binding procedure. This method was selected primarily for two reasons: its relatively low cost when compared to other commonly used wet chemical techniques such as Megazyme's amylose-amylopectin kit, and the procedure was reported to offer better precision than single wavelength iodine binding procedures (Zhu et al 2008). The method was modified to include a vortexing step during the dissolution of the starches. After collecting reference data for several samples, the validity of the reference data collected using the original procedure was questioned, because agglomerations (i.e., pockets of undissolved starch) were observed to readily form during the starch dissolution step of the method. Attempts to break up the agglomerations with a glass rod were not successful. Other treatments

such as sonication of sample flasks in an ultrasonic water bath did not resolve the issue either. The addition of vortexing during the starch dissolution step appeared to solve this issue. The measured amylose content of the 81 starch mixtures ranged from 0% to 23.2%. Negative values were obtained for the two pure waxy starches; however, these values were regarded as 0% amylose content, which had a negligible impact on the model results. All samples were measured at least twice. 57 samples met the stated limits of precision for inclusion in the calibration data. For selected samples that did not meet the stated limits for inclusion in the calibration data, the results from multiple runs of the same sample were pooled. The mean and standard deviation of the pooled data for a given sample were calculated, and values that were outside of 1 standard deviation were regarded as outliers. This was done because the data points for several samples appeared to have 1 or 2 outlying data points from the pooled data for a given sample. The remaining data points were averaged to find the mean amylose content of the sample. Taking these steps allowed another 10 samples to be included; 67 samples were available for use in the calibration and validation datasets. A summary of the datasets is shown in **Table 2.1**. By looking at the mean and standard deviation for the two datasets, the validation dataset appeared to be well representative of the calibration data.

Dataset	Amylose Range (%)	No. of Samples	Mean Amylose (%)	Standard Deviation (%)
Calibration	0.0 to 23.2	45	12.8	7.2
Validation	0.0 to 22.6	22	12.6	7.1

Table 2.1: Summary statistics of the calibration and validation datasets including all 67 samples that met precision standards.

Both partial least squares regression (PLS) and principal components regression (PCR) algorithms were used to model the data. A summary of the model results for the

calibration set detailed in **Table 2.1** is shown in **Table 2.2**. Generally speaking, the PLS models outperformed the PCR models; the PCR models required no less than 13 factors to obtain an SECV similar to that of the PLS models using fewer factors.

Algorithm	Region (cm^{-1})	Factors	r^2 (calibration)	SECV (%)
PLS	3200-250	7	0.801	3.23
PLS	2000-250	7	0.815	3.13
PLS	1500-250	8	0.814	3.21
PCR	3200-250	13	0.792	3.33
PCR	2000-250	13	0.807	3.19
PCR	1500-250	12	0.791	3.34

Table 2.2: Calibration model results of the calibration set detailed in Table 2.1.

Validation of the models showed poorer performance when using PCR when compared to PLS regression, leading to the study becoming primarily focused on the use of PLS regression. The result was not surprising; previous research has established that PLS is the primary multivariate method to be used for modeling Raman data to measure amylose content (Barton et al 2000; Himmelsbach et al 2001; Sohn et al 2004; Almeida et al 2010). It is worth noting that regression methods not available in the PLSplus/IQ software module have also been used with some success to model amylose data such as Martens' uncertainty regression (Sohn et al 2004). Truncating the spectral region of interest produced a small improvement in the calibration results of the PLS models. Attempts to remove obvious outliers from the calibration dataset were made by visually selecting data points that were far from the line of best fit for the instrument-predicted value vs. the experimental value of the calibration sample set. In some cases, this resulted in an improvement of the calibration results; however, subsequent validation of those models did not result in improvement of the validation results. Detection of

spectral outliers was performed by excluding any samples that exhibited a Mahalanobis distance greater than 3 as well as an F-test value larger than 0.99 as determined by PLSplus/IQ (Galactic Industries Corporation 1996). No spectral outliers were identified in the validation data. Additionally, use of other data preprocessing steps, like taking the first or second derivative of the calibration spectra using the Savitzky-Golay method, did not improve the calibration results. This may be because of the severely diminished intensity of important spectral features that would result from using such techniques, especially taking the second derivative, which could increase the impact of noise on the model results (Himmelsbach et al 2001). Additionally, some researchers suggested using the derivative of a given spectrum as an alternative to baseline correction (Almeida et al 2010). Since the spectra were baseline corrected using the Auto-Baseline function in the data collection software, it is unclear if also using derivatives could have contributed to the deleterious effect on the calibration results. The PLS calibration models displaying the best performance were examined more closely and validated against the validation dataset. The validation results for the two best models are shown in **Table 2.3**. The plot of actual vs. instrument-predicted values of the validation set using the 7-factor PLS model is shown in **Figure 2.2**. The plot of actual vs. instrument-predicted values of the validation set for the 8-factor PLS model is shown in **Figure 2.3**.

Algorithm	Region (cm^{-1})	Factors	r^2 (validation)	SEP (%)	Bias (%)	RPD
PLS	3200-250	7	0.812	3.05	-0.48	2.3
PLS	2000-250	7	0.831	2.90	-0.48	2.5
PLS	1500-250	8	0.845	2.85	-0.30	2.5

Table 2.3: Validation results of the PLS calibration models from Table 2.2.

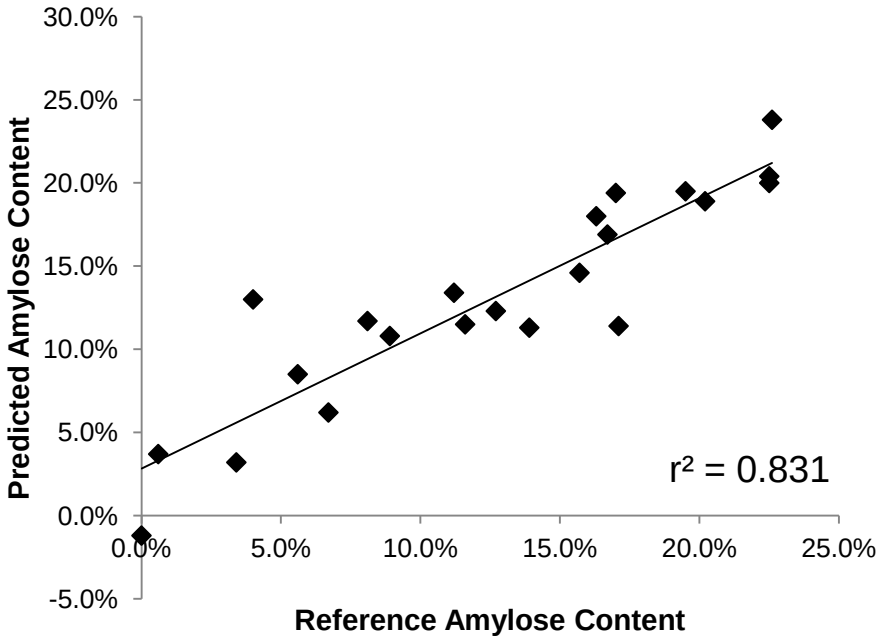

Figure 2.2: Plot of the instrument-predicted amylose content (2000 to 250 cm^{-1}) vs. the reference amylose content determined by iodine binding colorimetry. Samples were predicted using the 7-factor model described in Table 2.3.

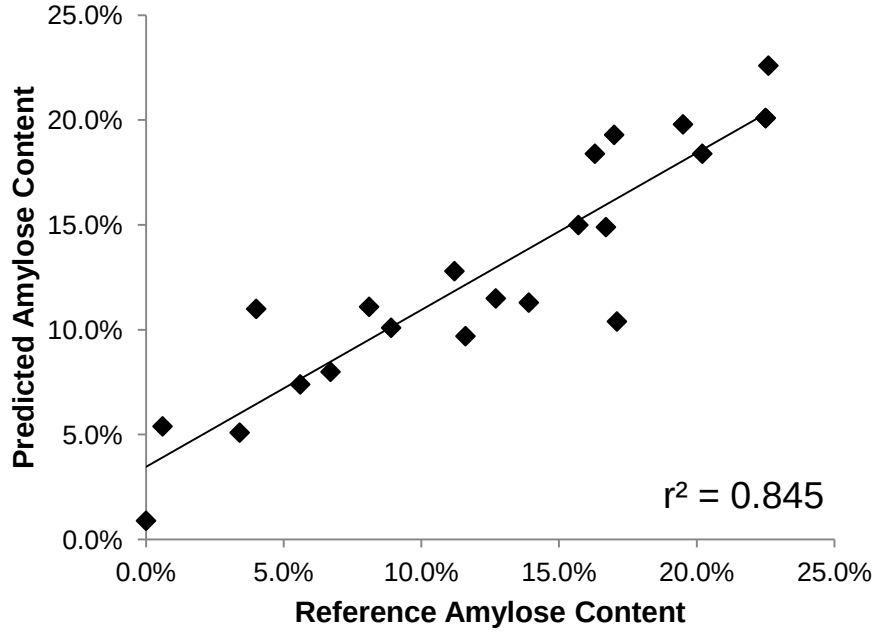

Figure 2.3: Plot of the instrument-predicted amylose content (1500 to 250 cm^{-1}) vs. the reference amylose content determined by iodine binding colorimetry. Samples were predicted using the 8-factor model described in Table 2.3.

Looking at the model results in **Table 2.3**, the most notable result is that the SEP is lower for both validated models than the SECV from the calibration models detailed in **Table 2.2**, indicating that the models perform reasonably well when measuring samples from the independent validation set. The model truncated to 1500-250 cm^{-1} had a slightly better r^2 of validation, SEP and bias than the model truncated to 2000-250 cm^{-1}, but not considerably so. Though a couple of data points from the validation set appeared to be outliers and were poorly predicted by both models, their sample spectra did not appear to be anomalous and thus were not excluded. Past researchers have obtained better model results when measuring amylose content of milled rice using FT-Raman spectroscopy with 1064 nm excitation, reporting SEP values as low as 1.05% (Himmelsbach et al 2001). Almeida et al (2010) reported that the band at 480 cm^{-1} is regarded as one of the most important in being able to measure amylose content; however, the researchers indicated that the band around 2900 cm^{-1} was also notable. As such, the poor signal for the band at 2900 cm^{-1} when using 785-nm excitation may have detracted from the overall ability of the models to measure amylose content. Another potential source of error in the samples is the relative precision and accuracy of methods that measure apparent amylose and the complexity of many of those techniques. In general, a spectroscopic method is regarded as only being as good as the reference data on which it is based. The bias for each of the two models was negative and would be regarded as large in some cases; however, the bias was relatively small compared to the SEP. By inspecting **Figures 2.2** and **2.3**, the sample measurements are observed to have a relatively even distribution above and below the line of best fit. Consideration of the RPD gives some

guidance on the potential implementation or use of the model for analytical purposes. Williams (2004) reported the scale shown in **Table A.3** in the appendix. These values were developed in reference to NIR methods, but the complementary nature of Raman and NIR spectroscopy would suggest that they have value when interpreting model performance results for Raman spectroscopy as well. An RPD value of 2.5 corresponds to a method recommended for "very rough screening" (Williams 2004).

The presence of NOVATION 4600, a waxy cold water swelling starch, in the validation and calibration datasets was also identified as a potential detractor to the overall performance of the models. The spectrum of this sample, as well as many of the spectra of samples containing this starch, was noisier in general but especially so in the region between 2000 and 250 cm^{-1}. Because this starch is not described as a modified starch, it is most likely a pregelatinized starch. Kim et al (1989) reported that gelatinizing starch resulted in a considerable decrease in intensity of most, if not all, Raman bands, especially the band at 480 cm^{-1}. This may be a possible cause of the spectral differences observed in this starch as compared to the other native starches that were studied. As such, samples containing NOVATION 4600 were removed from the dataset described in **Table 2.1**, and another dataset was constructed, shown in **Table 2.4**. Removing the samples containing the cold water swelling starch required removal of 17 samples from the original dataset, but the mean and standard deviation of the new dataset were quite similar to the original, only differing by a few tenths of a percent. Again, both PLS and PCR algorithms were used to model the data. The calibration results are shown in **Table 2.5**. All models detailed in **Table 2.5** were validated; the best validation results

for both the PLS and PCR algorithms are shown in **Table 2.6**. Interestingly, PCR became a more practical multivariate method for modeling the data once the cold water swelling starch was removed from the datasets, allowing for fewer factors to be used. However, PLS still outperformed PCR after validating two full spectrum calibration models (SEP = 2.70% for 5-factor PLS model, SEP = 2.92% for 9-factor PCR model). Additionally, the removal of the cold water swelling starch only nominally improved the validation results. Again, truncating the spectral region offered minor improvement in the validation results of the PLS models. All in all, removal of samples containing cold water swelling starch resulted in a minor improvement in model performance, but the overall performance of this method was not greatly improved. The relative performances of the models that include and exclude the cold water swelling starch demonstrates the robustness of the method, with several models being viable. Attempts to identify spectral outliers in the validation data (Mahalanobis distance **>** 3 and F-test value **>** 0.99) identified no spectral outliers for the models detailed in **Table 2.5**. Also, the ability of these models to identify samples containing cold water swelling starch was tested by measuring the amylose content of a starch mixture containing cold water swelling starch. The models were able to recognize these samples as spectral outliers based on the previously described criteria.

Dataset	Amylose Range (%)	No. of Samples	Mean Amylose (%)	Standard Deviation (%)
Calibration	0.0 to 23.2	34	11.8	7.5
Validation	1.7 to 22.5	16	12.2	7.1

Table 2.4: Summary statistics of the calibration and validation datasets excluding the cold water swelling starch, NOVATION 4600.

Algorithm	Region (cm^{-1})	Factors	r^2 (calibration)	SECV (%)
PLS	3200-250	5	**0.841**	**2.95**
PLS	2000-250	5	**0.843**	**2.93**
PLS	1500-250	5	**0.840**	**2.96**
PCR	3200-250	9	**0.838**	**2.97**
PCR	2000-250	3	**0.820**	**3.13**
PCR	1500-250	3	**0.825**	**3.09**

Table 2.5: Calibration model results of the validation set detailed in Table 2.4. Samples that included the cold water swelling starch, NOVATION 4600, are excluded from the calibration dataset from which these models were constructed.

Algorithm	Region (cm^{-1})	Factors	r^2 (validation)	SEP (%)	Bias (%)	RPD
PLS	3200-250	5	0.860	2.70	0.49	2.6
PLS	2000-250	5	0.874	2.58	0.58	2.8
PLS	1500-250	5	0.870	2.60	0.53	2.7
PCR	2000-250	9	0.832	2.92	0.58	2.4

Table 2.6: Best validation results for calibration models detailed in Table 2.5. Samples that included the cold water swelling starch, NOVATION 4600, are excluded from the calibration and validation datasets.

Finally, three different calibration datasets were also prepared based on excluding samples of "low" amylose content, or rather samples that were below 8%, 10% and 15% amylose content as measured by the reference method, respectively. This was done to test whether separate models for "high" amylose content may better model the data. While doing so improved the SECV for the calibration models due to the smaller range of amylose contents being measured, the r^2 of calibration was not improved in any of the calibration models. Moreover, validation of selected models from these datasets showed poorer performance than the models from the original expanded dataset.

Conclusions

Models generated using a portable instrument and 785-nm excitation did not perform as well as those obtained by previous researchers using a research-grade FT-

Raman instrument with 1064-nm excitation. While the results for quantifying amylose content were not as good, this method is easily capable of discriminating between waxy and normal starches. This offers the potential for the development of this technique to be utilized in other ways than measuring percent amylose content. For example, this method could have potential as a screening tool to identify starch shipments as waxy and normal. Moreover, Sohn et al (2004) reported drastically improved calibration results after applying orthogonal signal correction (OSC) as a preprocessing step for an FT-Raman spectroscopic method for measuring amylose content of rice flour. Sophisticated data preprocessing such as OSC may be able to be used to similar effect with the more portable and inexpensive dispersive Raman spectroscopic instruments. Moreover, preprocessing steps not available in the software package used in this study may also offer some improvement in model performance and should be explored. The model results demonstrated that the method is robust, with several models showing relatively similar performance in spite of model parameters being varied. Inexpensive instrumentation such as dispersive Raman spectrometers may have potential as an alternative to wet chemical techniques for measuring amylose content of starches. Future work should include examining the performance of the models after application of other preprocessing steps and possibly repeating the experiment with NIR spectroscopy to determine how the two techniques compare.

References

Almeida, M. R., Alves, R. S., Nascimbem, L. B. L. R., Stephani, R., Poppi, R. J., and de Oliveira, L. F. C. 2010. Determination of amylose content in starch using Raman spectroscopy and multivariate calibration analysis. Anal. Bioanal. Chem. 397:2693-2701.

Barton, F. E., Himmelsbach, D. S., McClung, A. M., and Champagne, E. T. 2000. Rice quality by spectroscopic analysis: precision of three spectral regions. Cereal Chem. 77:669-672.

Bates, F. L, French, D., and Rundel, R. E. 1943. Amylose and amylopectin content of starches determined by their iodine complex formation. J. Am. Chem. Soc. 65: 142-148.

Bertoft, E. 2004. Analysing Starch Structure. Pages 57-96 in: Starch in food: Structure, function and applications. A.-C. Eliasson, ed. CRC Press: Boca Raton.

Fitzgerald, M. A., Bergman, C. J., Ressurreccion, A. P., Moller, J., Jimenez, R., Reinke, R. F., Martin, M., Blanco, P., Molina, F., Chen, M., Kuri, V., Romero, M. V., Habibi, F., Umemoto, T., Jongdee, S., Graterol, E., Reddy, K. R., Bassinello, P. Z., Sivakami, R., Rani, N. S., Das, S., Wang, Y., Indrasari, S. D., Ramli, A., Ahmad, R., Dipti, S. S., Xie, L., Lang, N. T., Singh, P., Toro, D. C., Tavasoli, F. and Mestres C. 2009. Addressing the dilemmas of measuring amylose in rice. Cereal Chem. 86:492-498.

Galactic Industries Corporation. 1996. Appendix B. Pages 180-181 in: PLSplus/IQ User's Guide. Galactic Industries Corporation: Salem.

Himmelsbach, D. S., Barton, F. E., McClung, M. A., and Champagne, E. T. 2001. Protein and apparent amylose contents of milled rice by NIR-FT/Raman spectroscopy. Cereal Chem. 78:488-492.

Jarvis, C. E., and Walker, J. R. L. 1993. Simultaneous, rapid, spectrophotometric determination of total starch, amylose and amylopectin. J. Sci. Food Agric. 63:53-57.

Johnson, L. A., Baumel, C. P., Hardy, C. L., and White, P. J. 1999. Identifying Valuable Corn Quality Traits for Starch Production. Iowa State University Extension: Ames. Available online at: http://www.extension.iastate.edu/Publications/EDC194.pdf.

Kim, I.-H., Yeh, A., Zhao, B. L., and Wang, S. S. 1989. Gelatinization kinetics of starch by using Raman spectroscopy. Biotechnol. Prog. 5:172-174.

Larson, B. L., Gilles, K. A., and Jenness, R. 1953. Amperometric method for determining the sorption of iodine by starch. Anal. Chem. 25:802-804.

Phillips, D. L., Xing, J., Liu, H., Pan, D.-H., and Corke, H. 1999. Potential use of Raman spectroscopy for determination of amylose content in maize starch. Cereal Chem. 76:821-823.

Satin, M. 2000. Functional Properties of Starches. FAO Agriculture and Consumer Protection Department: Rome. Available online at: http://www.fao.org/ag/magazine/pdf/starches.pdf

Sohn, M., Himmelsbach, D. S., and Barton, F. E. 2004. A comparative study of Fourier transform Raman and NIR spectroscopic methods for assessment of protein and apparent amylose in rice. Cereal Chem. 81: 429-433.

Wang, J. P., Li, Y., Tian, Y. Q., Xu, X. M., Ji, X. X., Cao, X., and Jin, Z. Y. 2010. A novel triple-wavelength colorimetric method for measuring amylose and amylopectin contents. Starch/Starke 62:508-516.

Wang, T. L., Bogracheva, T. Y., and Hedley, C. L. 1998. Starch: as simple as A, B, C?. J. Exp. Bot. 49:481-502.

Williams, P. C. 2004. Implementation of Near-Infrared Technology. Pages 145-169 in: Near-Infrared Technology in the Agricultural and Food Industries. P. Williams and K. Norris, eds. American Association of Cereal Chemists, Inc.: St. Paul.

Zhu, T., Jackson, D. S., Wehling, R. L., and Geera, B. 2008. Comparison of amylose determination methods and the development of a dual wavelength iodine binding technique. Cereal Chem. 85:51-58.

Chapter III:
DEVELOPMENT OF A RAMAN SPECTROSCOPIC METHOD FOR MEASURING RETROGRADATION IN CORN STARCH GELS

Abstract

A study utilizing Raman spectroscopy to monitor starch retrogradation in corn starch gels was performed. Starch retrogradation is the process by which gelatinized starch will undergo a series of physical and chemical changes as it ages, resulting in often undesirable qualities in starch-based foods. As such, retrogradation is a primary source of quality degradation in starch-based food products in the food industry. Many existing methods are available for measuring retrogradation in starch-containing foods; however, much of the existing methodology is destructive to the sample or requires expensive instrumentation. Raman spectroscopy may be able to offer a rapid, portable and non-destructive alternative to the existing techniques. Six series of starch gels (10% w/v) were prepared from three sources of normal corn starch (2 series of gels per source, 6 gels per series) by heating starch slurries in capped 35-ml centrifuge tubes in a hot water bath at about 90° C for 90 min, resulting in 36 total gels. Each gel was stored at 4° C and measured at regular intervals (0 h, 24 h, 48 h, 72 h, 120 h, 168 h after preparation) over the region of 250 cm^{-1} to 3200 cm^{-1} using an Enwave Optronics EZRaman-M series Raman spectrometer with an excitation wavelength of 785 nm. Scanning parameters were optimized, with a 30 second integration time and collection of a single scan found to give suitable results. Duplicate scans were made by rotating the vials 90° between scans. Gels were frozen, freeze-dried, equilibrated to approximately equal moisture levels and measured using X-ray diffraction. The relative crystallinity of each freeze-dried gel was determined using two different methods and correlated with intensity changes in the Raman band at 480 cm^{-1} measured using three different methods. No correlation was

found between the reference data and the intensity changes of the band at 480 cm^{-1} using any of the methods ($r^2 < .1$). The ultimate goal of this research is to develop a Raman spectroscopic method for measuring retrogradation in a model food product like white pan bread; however, more development is needed.

Introduction

Starch, a widely used food ingredient, has many functional properties, and its ability to form gels and thicken mixtures is commonly exploited in the food industry. For example, starch gelling makes the production of puddings, pie fillings and many sauces possible (Satin 2000). Additionally, starch, as a component of flour, undergoes gelatinization during bread making, with an estimated 20 billion pounds of bread being produced annually (Zobel and Kulp 1996). As a physicochemical process, gelatinization involves the heating and dispersion of starch in water, during which starch granules swell and may burst. The result of this process is leaching of amylose from starch granules and a loss of crystallinity, forming a gel (Keetels et al 1996; Donald 2004). With time, a process known as retrogradation also occurs, and this progression is commonly implicated as a primary cause of quality deterioration in starch-based products, particularly in the staling of bread and other baked goods, which can occur prior to other types of degradation like fungal or bacterial growth. During retrogradation, starch chains begin to partially recrystallize, allowing for incomplete restoration of crystalline order at the molecular level and causing increased textural firmness and moisture loss in starch-based products (Gudmundsson 1994; Keetels et al 1996; Zobel and Kulp 1996). This kind of quality degradation in starch-containing products is known to become more

severe and increasingly detectable as the products continue to age (Gudmundsson 1994; Zobel and Kulp 1996).

Numerous methods are available to measure retrogradation in starch-based products. Generally speaking, two categories of methods exist: macroscopic and molecular (Karim et al 2000). Macroscopic methods can be used to measure physical changes such as textural firming, while molecular methods are utilized to directly measure changes at the molecular level like variations in the relative crystallinity of a product (Karim et al 2000). X-ray diffraction, a molecular technique, has long been used by academia to research crystal structures; methods have also been developed that allow for the estimation of the relative proportions of crystalline and amorphous phases of a powdered starch sample (Nara et al 1978; Karim et al 2000). Such methods allow investigators to monitor processes like retrogradation in starch gels and its impact on crystallinity in starch-based food products, like bread (Kim et al 1997; Karim et al 2000; Ribotta et al 2004). Generally speaking, the high cost of instrumentation and maintenance associated with many molecular methods may limit their widespread use in the food industry, where macroscopic methods like differential scanning calorimetry, texture analysis and sensory evaluation may be more commonly used to detect quality degradation caused by retrogradation. However, molecular methods may grow in popularity with time and more research, as some of these methods, like Raman spectroscopy, have the potential to offer inexpensive, rapid and non-destructive alternatives to macroscopic methods.

Very little research has been done on using Raman spectroscopy to measure retrogradation in starch gels, and a similarly small body of research has been conducted on using Raman spectroscopy to measure retrogradation in a model food product. Researchers have demonstrated that small yet measurable changes occur in the wavenumber position and full-width at half height of the Raman bands at 480 cm^{-1} and about 2900 cm^{-1} (Bulkin et al 1987; Fechner et al 2005). Each of these studies looked at the retrogradation kinetics of starches from various sources but did not correlate the spectral data with any accepted reference method. Some work has been done using Raman spectroscopy to monitor retrogradation in finished food products such as semolina-based sourdough bread (Piccinini et al 2012) and tortillas (Flores-Morales et al 2012). Only one of these studies correlated their findings with measurements from a commonly used reference method (Piccinini et al 2012). The researchers observed a strong linear association ($r^2 > .9$) between the full width measured at half height of the Raman band at 480 cm^{-1} and bread crumb hardness each measured over a period of 20 days (Piccinini et al 2012). Thus, little research has looked at correlating the results of a reference method with peak changes in Raman data. To address this gap in the literature, the objective of this study was to develop and assess the usefulness of an inexpensive Raman spectroscopic method for continuous measurement of retrogradation in corn starch gels over time.

Materials and Methods

Sample preparation

Preliminary experiments revealed that a 10% (w/v) starch gel was optimal for sample handling for both the Raman spectroscopic data collection and the reference data collection; therefore, 10% starch gels were prepared. Three sources of normal corn starch were used: a local store brand (HyVee), Argo (ACH Food Companies, Memphis, TN) and National Starch (Bridgewater, NJ) MELOJEL. Three gel series were prepared and duplicated so that measurements could be made at 6 time intervals (immediately after the gels had cooled to ambient temperature (0 h) or 24 h, 48 h, 72 h, 120 h and 168 h after gels were prepared). Using two separate centrifuge tubes for each individual starch source at each time interval, 12 total gels were prepared from each starch source for a total of 36 samples. Each gel was measured at only one predetermined time interval, and all gels in a series were prepared simultaneously. Distilled water (500 ml) was added to a 600-ml beaker, and the beaker was placed on a stir plate after which a magnetic stir bar was added to the water. The stir plate's speed was set to 50% of maximum. A top-loading balance was used to weigh 50 g of starch into a weigh boat, and then the starch was carefully and slowly added to the stirring water on the stir plate to allow thorough dispersal. Once all of the starch was dispersed, the stir plate's speed was increased to about 75% of maximum to facilitate constant suspension of the starch. A 25-ml volumetric pipette was used to transfer 25 ml of the starch slurry to a 35-ml KIMAX (Kimble-Chase, Vineland, NJ) centrifuge tube. The tubes were labeled according to their starch source, duplicate number, and the number of days the tube was to be stored, and then sealed with the provided screw-caps. A hot water bath (90 °C) was used to heat the

samples. Before placing the starch slurries into the hot water bath, each tube was vortexed at maximum speed for several seconds to suspend any starch that had settled. The tubes were heated for 90 min to ensure full gelatinization. Every 10 min, each tube was removed and inverted several times to resuspend any settled starch and then placed back in the water bath. After the heating time had elapsed, the tubes were removed from the bath and allowed to cool for 45 min at ambient temperature. Gels were monitored using Raman spectroscopy over a period of 7 days following their preparation. Spectral measurements were made immediately after preparation as well as 24 h, 48 h, 72 h, 120 h and 168 h after preparation. Gels were stored at refrigeration temperature (4 °C) until scans were made at each time interval. Amorphous standard samples were prepared for use in the X-ray diffraction measurements using a similar protocol, as described in the following paragraph.

Preparation of amorphous phase standards

Amorphous phase standards were prepared using a modified version of the procedure described by Ratnayake and Jackson (2008) for preparing starch gel samples. Two 10% starch gels were prepared by slurrying 10 g of Argo corn starch in 100 ml of distilled water in a 250-ml beaker on a stir plate, then using a 25-ml volumetric pipette to fill KIMAX 35-ml centrifuge tubes with starch slurry, and heating samples in a 400-ml beaker of hot water (95 °C) for 90 min. Sample tubes were removed every 10 min and inverted several times to resuspend any starch that had settled and then placed back in the beaker of hot water. Next, excess water was removed from each starch paste by draining through Whatman No. 1 filter paper using gravity, and the gels were then transferred to

individual 50-ml plastic centrifuge tubes and placed in a freezer at -80 °C. A meat thermometer was used to measure the internal temperature of one gel. After 30 min, the gel being monitored reached 0 °C or lower. Then, the samples were freeze-dried for 48 h (-52 °C at 0.051 Torr).

Raman spectroscopy

All Raman spectral data were collected using an Enwave Optronics (Irvine, CA) EZRaman-M series Raman spectrometer connected to a laptop computer. The EZRaman Reader software provided with the Raman analyzer was used to handle the data collection. Sample spectra were measured over the region of 250 cm^{-1} to 3200 cm^{-1} with an optical resolution of 6 cm^{-1} using the instrument's remote probe attachment. The excitation wavelength of the laser was 785 nm, while the power of the laser was set at approximately 300 to 400 mW. Preliminary experiments showed that a measurement distance of about 3 mm provided the best quality spectrum. A 3.175-mm thick rubber washer purchased from a local hardware store was used as a spacer so that the distance between the sample tube and the remote probe lens was kept constant. Before scanning, sample tubes were cleaned with a KimWipe to remove any fingerprints or residues that may interfere with data collection. Preliminary experiments revealed that the optimal scanning parameters were an integration time of 30 s, collection of a single scan, and a smoothing level of 1. Duplicate scans were achieved by rotating each centrifuge tube 90° between scans.

Sample preparation for X-ray diffraction

After spectral measurements were made, samples from each time interval were immediately placed in a freezer and held overnight at about -20 °C for 19 h to ensure samples were completely frozen. Because some retrogradation may have occurred while samples were freezing, Raman spectral measurements were also made on gels in the frozen state after removal from the freezer using the previously described parameters. Samples were lyophilized at -52 °C and 0.051 Torr for 48 h using a LABCONCO (Kansas City, MO) FreeZone freeze-dryer. The dried gels were broken up using a spatula and ground into a powder using a mortar and pestle. Dried gels were transferred to labeled septum-fitted vials and stored in a desiccator until all samples were ready for moisture equilibration. Once all samples were prepared, the moisture contents of all samples were equilibrated by storing the samples in a sealed chamber. Three 600-ml beakers were filled with distilled water and placed on the bottom shelf of a vacuum oven. Each sample was transferred to a disposable Petri dish, and the powder was spread in a thin layer along the bottom of the plate. The vacuum oven was sealed, and the samples were stored in this manner for 48 h. A digital hygrometer was used to determine the relative humidity inside the oven. Preliminary experiments revealed that storing samples like this for 48 h resulted in an end moisture content of about 20% (wet basis). After 48 h, the Petri plates were removed from the oven, and the samples were transferred back to labeled septum-fitted vials and stored at approximately -20 °C in a freezer until X-ray measurements were made.

X-ray diffraction

X-ray measurements were made using a procedure described by Ratnayake and Jackson (2008) with minor modifications to the scan and integration conditions. Samples were mounted on aluminum sample plates by using a Pasteur pipette to place a couple of drops of ethanol into each sample well, followed by the freeze-dried and ground starch samples, and then compaction with a glass slide to provide a smooth surface for measurement (Ratnayake and Jackson 2008). The X-ray diffractometer used for this study was a Bruker-AXS D8 Discover system (Bruker AXS GmbH, Karlsruhe, Germany) with a general area detector diffraction system (GADDS). A copper target X-ray tube was used to make the X-ray measurements. The instrument was equipped with a Göbel mirror and a HI-STAR area detector. The X-ray tube was set to 40 kV and 40 mA. The scan conditions were omega = 4°, detector swing angle = 18°, sample to detector distance = 10.1 cm and an exposure time of 180 s (Ratnayake and Jackson 2008). Frame data were integrated over 2 theta = 3 to 35° and chi = -130 to -50° using the GADDS data collection software provided with the instrument (Ratnayake and Jackson 2008). Because of the high frequency of samples falling out of the sample mount before or while scans were being made, each sample was only measured once. Percent relative crystallinity (see **Equation 3.1**) and estimated relative crystallinity were calculated according to the methods described by Ratnayake and Jackson (2008) and Kim et al (1997), respectively. Estimated relative crystallinity was calculated by finding the ratio of the area of the crystalline peaks to the area of the entire diffractogram between 2-theta = 7 to 35° (Kim et al 1997). When calculating estimated relative crystallinity, the peak

between 2-theta = 3 to 7° in the diffractograms was excluded from the calculations due to its low intensity and poor resolution.

Spectral preprocessing and data analysis

Spectral preprocessing such as linearization, baseline correction, and averaging of replicate scans was performed in GRAMS/AI 8.0 (Thermo Scientific, Woburn, MA). For all Raman spectra, a 4-point baseline was created using the baseline correction function in GRAMS/AI 8.0. Baseline correction of diffractograms and crystalline peaks in the diffractograms, additional smoothing of Raman spectral data, integration of spectral and diffractogram peaks, and calculation of the absolute difference between X-ray diffractograms, according to **Equation 3.1**, was performed in Origin Pro v8.6 (OriginLab Corporation, Northampton, MA). All other calculations, including percent relative crystallinity and estimated relative crystallinity, were made using Microsoft Excel 2007.

Equation 3.1: $\%\ Relative\ Crystallinity = (\sum|I_s - I_a|/\sum|I_c - I_a|) \times 100\%$, where $|I_s - I_a|$ is the absolute difference between the sample [I_s] and amorphous [I_a] intensities and $|I_c - I_a|$ is the absolute difference between the crystalline [I_c] and amorphous [I_a] intensities (Ratnayake and Jackson 2008).

Results and Discussion

Several procedures were tested to determine the optimal techniques for preparing and measuring starch gels. Preliminary experiments revealed that a 10% (w/v) starch gel was optimal for sample handling and preparation and was regarded as satisfactory for the Raman method and the X-ray diffraction reference method. Past experiments looking at retrogradation of starch gels prepared from various cereal and root sources suggested that high concentrations of starch (≥ 45% w/w) allowed for a sufficiently strong Raman signal

and the researchers' desired closely-packed system to monitor the phenomenon's kinetics (Bulkin et al 1987; Fechner et al 2005). Additionally, past research that used Raman spectroscopy with visible light excitation to examine gelatinization kinetics of starch showed that gelatinized starch had greatly diminished signal strength at most of the commonly reported Raman bands following gelatinization (Kim et al 1989). Due to this, the feasibility of using more concentrated (>10% w/v) starch gels was examined in preliminary experiments, but higher concentrations proved to be excessively difficult to use with the selected reference data collection method, with starch gels being very firm in texture after freeze-drying and thus problematic to grind into a powder with a mortar and pestle.

Preliminary experiments revealed that the optimal Raman scanning parameters were an integration time of 30 s, collecting 1 scan per tube, and a smoothing level of 1. Using longer integration times and averaging of additional scans per tube did not offer considerable improvement in the noise level of the sample spectra. In fact, increases in these two scanning parameters appeared to increase the noise level of the sample spectra. Rather than using the option included in the data collection software, any additional smoothing of sample spectra was applied during data analysis, allowing for better control of this parameter. Several types of sample containers were tested including VWR short-form style 1.8-ml sample vials, KIMAX 35-ml centrifuge tubes and beakers of varying volume. The Raman signal was expected to be somewhat degraded due to the gelatinization of the starch (Kim et al 1989); however, the commonly reported Raman bands were of weak intensity and not well resolved with any of these containers.

Although, two bands were more noticeable when using the centrifuge tubes. As shown in **Figure 3.1**, the only Raman bands typically associated with starch that were visible in the gelatinized samples were the C-H stretching band at about 2910 cm^{-1} and the band at 480 cm^{-1}, a band associated with "skeletal mode" vibrations (Almeida et al 2010; Piccinini et al 2012). Neither of these bands were of strong intensity or well resolved. The exact cause of the broad spectral feature between 1000 and 2700 cm^{-1} is unknown. Raman scans of an empty KIMAX centrifuge tube using the scanning parameters previously described revealed a similar broad spectral feature in this region but of much weaker intensity, and it remains unclear if the sample container contributed to this. The sharp peak around 890 cm^{-1} appeared to be a contribution from noise, as it does not appear in all of the spectra from a given gel series.

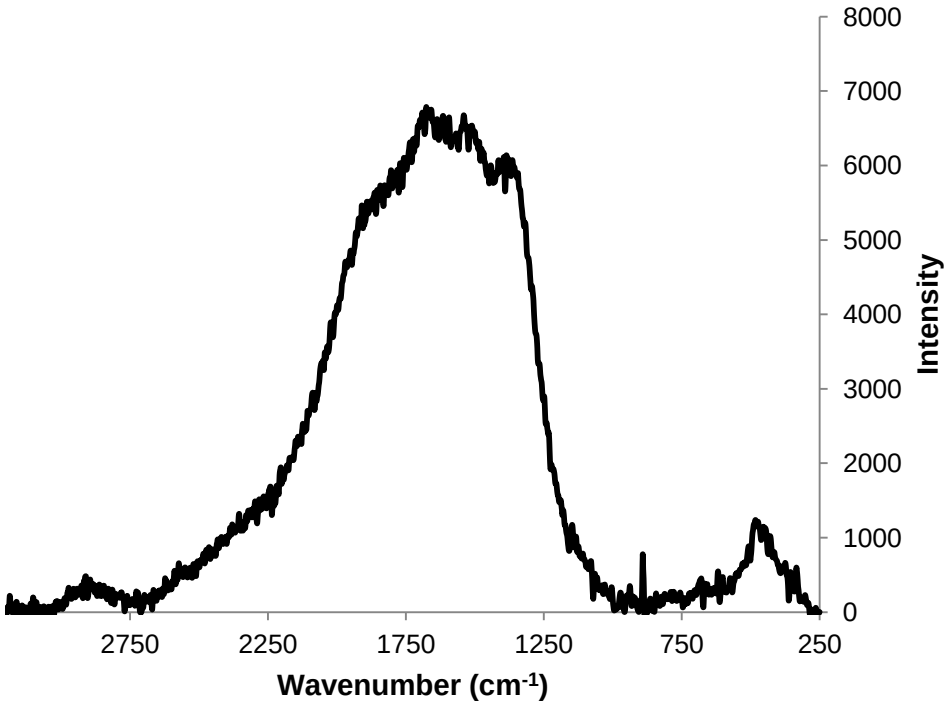

Figure 3.1: Raman spectrum between 3200 and 250 cm^{-1} of gelatinized Argo corn starch cooled for 45 min (t = 0 h) after cooking for 90 min. Spectrum is the average of two sample scans; replicates were achieved by rotating the sample centrifuge tube 90° between scans.

A modified version of the X-ray diffractometry technique for determining percent relative crystallinity described by Ratnayake and Jackson (2008) was utilized to collect reference data for the study. Percent relative crystallinity was determined for 34 samples. Values were not determined for two prepared samples due to improper drying that resulted in one sample being discarded and a software error that resulted in loss of diffractogram data for another. The measured relative crystallinity of the 34 samples ranged from 4.9 to 25.3%, with a mean of 12.6% and a standard deviation of 3.6%. When comparing the data with storage time, the measured relative crystallinity did not increase in a predictable pattern for all samples. **Figure 3.2** shows a comparison of the percent relative crystallinity with the storage time in hours for one gel series prepared

from Argo corn starch. As retrogradation occurs, starch chains recrystallize, resulting in an increase in the relative proportion of the crystalline phase to the amorphous phase over time. However, this relationship was not observed consistently in any of the reference data generated for the starch gels when calculating percent relative crystallinity using the method described by Ratnayake and Jackson (2008). Repeating the calculations but excluding the poorly resolved peak between 2-theta = 3 to 7° from each diffractogram did not have any impact on the relationship between the storage time and the relative crystallinity. As such, another method for calculating relative crystallinity was examined. The method described by Kim et al (1997) was employed, which involved integrating the area under the crystalline peaks in the diffractogram and determining the ratio of that area to the area of the entire diffractogram. Using this method, diffractograms were only analyzed from 2-theta = 7 to 35° because the peak between 3 and 7° did not appear to be well resolved. Using this method, the estimated relative crystallinity for the gels ranged from 3.4 to 5.8%, with a mean of 4.2% and a standard deviation of 0.6%. **Figure 3.3** shows a comparison of the estimated relative crystallinity (%) the storage time in hours for the same gel series depicted in **Figure 3.2**.

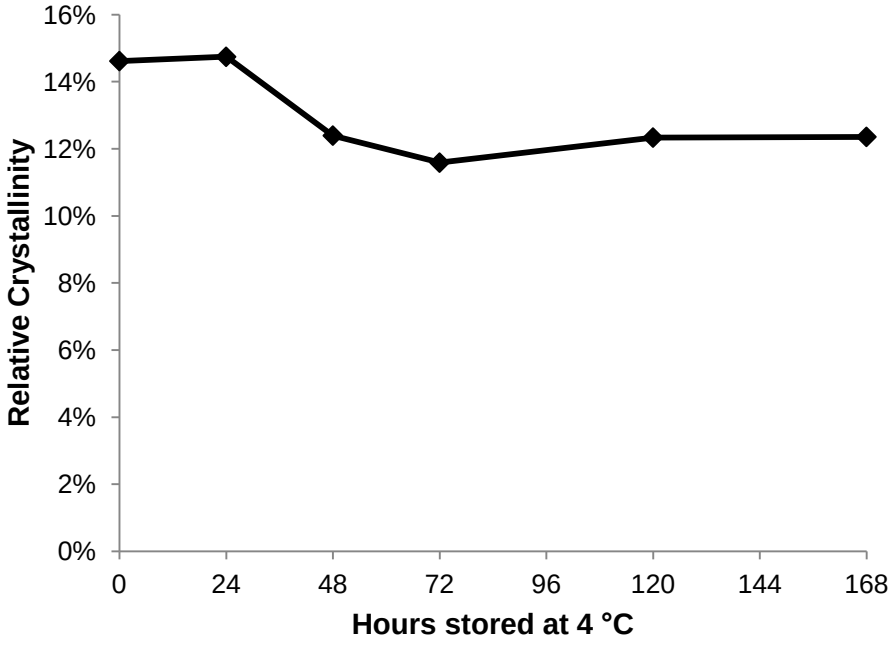

Figure 3.2: Plot comparing relative crystallinity with storage time in hours for one gel series prepared from Argo corn starch. Relative crystallinity was determined using the method described by Ratnayake and Jackson (2008).

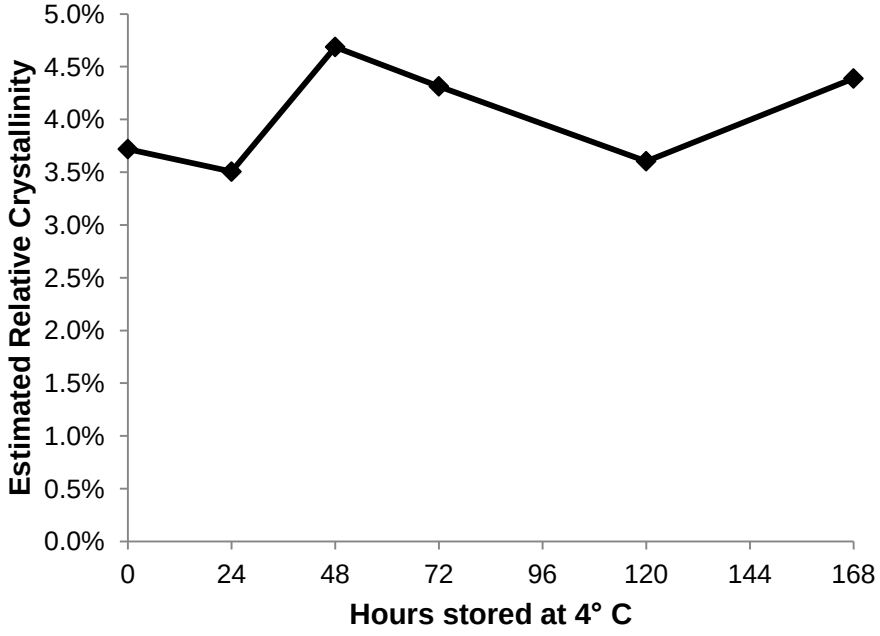

Figure 3.3: Plot comparing estimated relative crystallinity with storage time in hours for one gel series prepared from Argo corn starch. Values depicted are for the same gel series depicted in Figure 3.2. Estimated relative crystallinity was determined using the method described by Kim et al (1997).

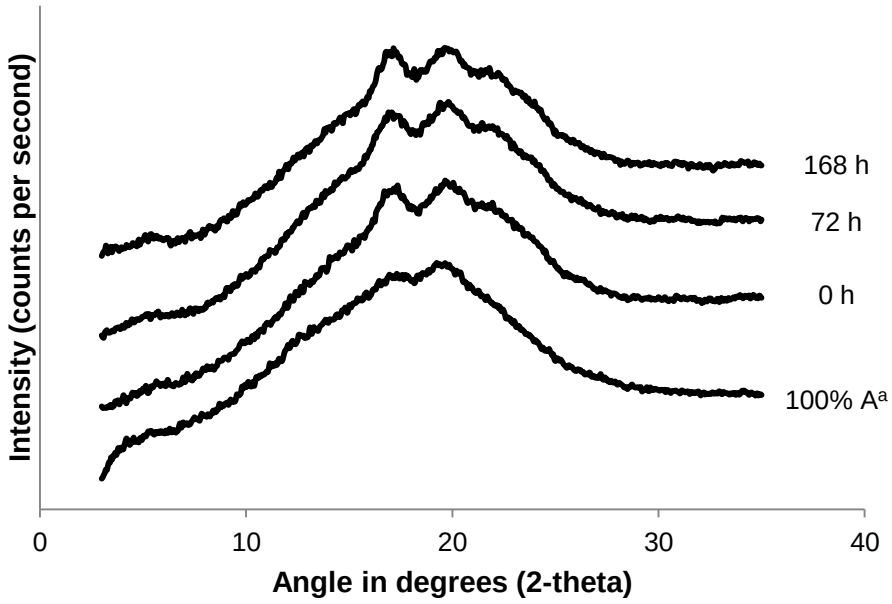

Figure 3.4: Diffractogram comparison of data from one gel series to the amorphous standard sample that was prepared. Intensity (y-axis) is not to scale. The labels next to each diffractogram refer to the storage time at 4 °C for each sample; [a]100% A refers to the diffractogram for a 100% amorphous standard.

As with the previous method, the estimated relative crystallinity did not appear to increase in a manner consistent with that which was expected from starch retrogradation. **Figure 3.4** shows a comparison of X-ray diffractograms, between 2-theta = 3 to 35°, from one gel series prepared from Argo corn starch. Visual inspection of each diffractogram in **Figure 3.4** shows considerable differences in the size of the crystalline peaks at about 17 and 19.5° when comparing the amorphous standard and any of the three diffractograms from varying time intervals; however, these peaks do not appear to differ very much or at all among the three diffractograms from varying time intervals. It is worth nothing that Kim et al (1997) reported in a comparison study of three methods for measuring retrogradation in rice starch gels that X-ray diffraction was the least sensitive of the methods tested, requiring the starch in the gel to be "considerably

recrystallized" to observe peaks. As such, the low amount of retrogradation that occurred may not be accurately detectable by the chosen reference method. The lack of substantial peak differences in the diffractograms shown in **Figure 3.4** could have a couple of explanations. Amylose has been reported to recrystallize more rapidly than amylopectin (Lai et al 2000). As such, the crystalline peaks observed in the diffractograms may have been caused by the rapid recrystallization of amylose upon cooling of the starch gels. Additionally, the slower recrystallization of amylopectin over time may have been hindered by the dilute starch concentration used in the study (Zeleznak and Hosney 1986). As such, crystalline peaks were observed, but the relationship with storage time was not linear.

The relatively poor signal-to-noise ratio of the spectral data mostly precluded the use of multivariate data analysis methods. Due to this and the poor resolution and signal strength of the peak around 2910 cm^{-1}, monitoring intensity changes of the peak at 480 cm^{-1} became the focus of the study. Previous research has indicated that the intensity of this band is greatly diminished after gelatinization (Kim et al 1989); however, other studies looking at retrogradation have indicated that this band will show small changes in the full-width at half-height of the band and begin to sharpen as the starch recrystallizes (Bulkin et al 1987; Fechner et al 2005; Piccinini et al 2012). Preliminary experiments showed that this peak appeared to increase in intensity or become sharper relative to other persistent features in the spectrum (i.e., valleys or other peaks of weak intensity) as the gels aged. **Figure 3.5** shows the Raman spectra of a series of gels prepared from Argo corn starch and measured at varying time intervals. Visually inspecting the region around

480 cm^{-1} appeared to show an increase in intensity or sharpening of the band with time relative to the surrounding features. This change was not observed in each gel series, though. Because of the tiny degree of change reported in the literature at the band at 480 cm^{-1} over longer time studies than the time period used in this study, the method reported by previous researchers of tracking the full-width at half-height of the 480 cm^{-1} band was not investigated (Bulkin et al 1987; Fechner et al 2005; Piccinini et al 2012). Instead, three methods were employed to measure the intensity changes in the band at approximately 480 cm^{-1}. First, the difference between the intensity of the band around 480 cm^{-1} and the intensity of a valley at its lowest point between 499 and 503 cm^{-1} was calculated. As with the diffractogram data, the results were inconsistent with the expected result; the band differences did not increase in a predictable fashion. Because the noise level was considerable, using Origin Pro v8.6., the spectral data was smoothed using the software's Savitzky-Golay filtering (20 points of window), and additional parameters were left as their default options. Then, a baseline was drawn between 460.6 and 507.4 cm^{-1}. These wavenumbers were selected because they correspond to two valleys in the spectrum whose wavenumber positions shifted very little between samples. The area under the peak, the peak height at maximum intensity and the wavenumber value at maximum intensity were determined. Using this method, the results were again unpredictable; within a given gel series, some samples at earlier time intervals (24 or 48 h) had a higher intensity or peak area than samples held for longer time intervals. Finally, to normalize the peak area of the band at 480 cm^{-1}, the ratio of the integrated peak area between 460.6 and 507.4 cm^{-1} and the integrated peak area between

approximately 270 to 590 cm^{-1} for the smoothed spectral data was determined. The wavenumbers at 270 and 590 cm^{-1} were selected because they corresponded to two valleys in the spectrum that shifted only a few wavenumbers between samples. As with the other methods, the relative change in the ratio of these areas did not change consistently for all gel series, with some gel series having a larger ratio at intermediate time intervals (72 h) than at the later time intervals (120 h or 168 h).

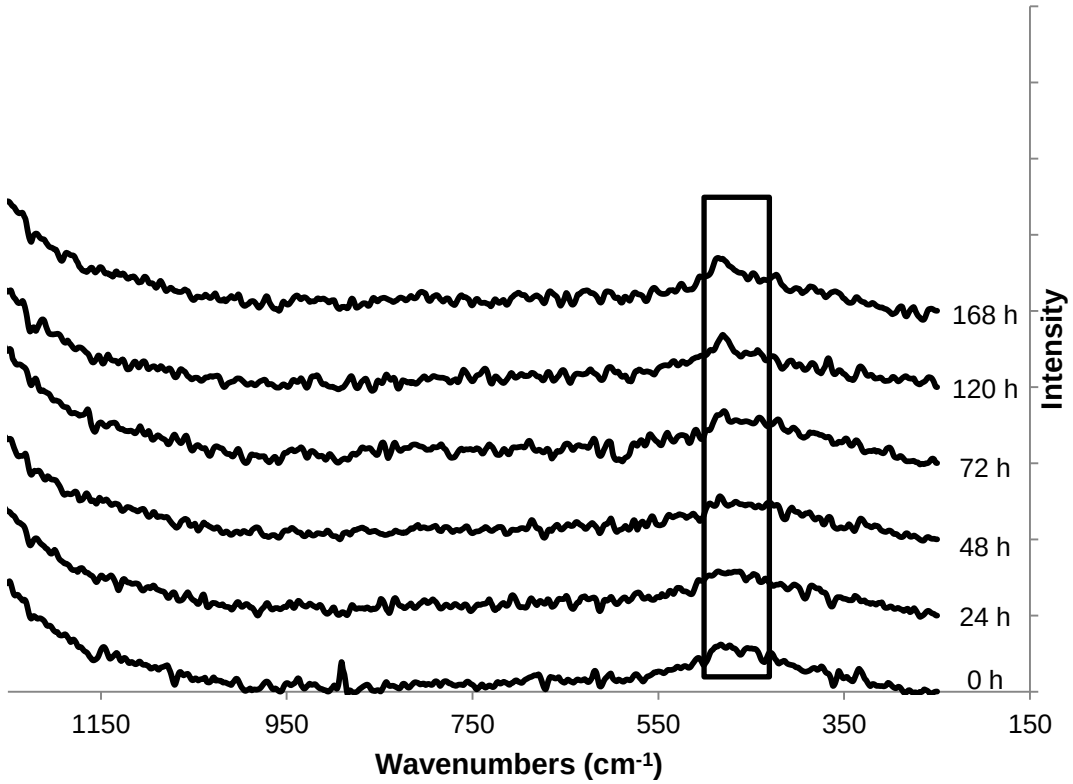

Figure 3.5: Comparison of Raman spectral data from a gel series prepared from Argo corn starch. Intensity is not to scale. The spectral region within the rectangle indicates the relative position of the band around 480 cm^{-1}.

Attempts to correlate the intensity data calculated using these three methods with the reference data calculated using the two previously described methods resulted in poor values for the coefficient of determination ($r^2 < .1$). As before with the X-ray diffraction

data, the Raman instrument may not be sensitive enough to measure retrogradation in gels that are very dilute. Past studies looking at retrogradation kinetics were done on gels of concentrations no less than 40% (Bulkin et al 1987; Fechner et al 2005). The concentration dependence of retrogradation reported by Zeleznak and Hoseney (1986) may have contributed as well, in which the authors noted that little crystallinity was present in 20% (w/w) wheat starch gels measured by DSC.

Conclusions

The applicability of Raman spectroscopy to measuring retrogradation in starch gels may be problematic at dilute concentrations. The X-ray diffraction and Raman spectral data exhibited a poor coefficient of determination when attempts were made to correlate the data, showing there was essentially no correlation between the data. Use of a higher starch gel concentration may be necessary to better observe starch retrogradation with Raman spectroscopy. Holding gels for a longer time period than 7 days may also be necessary, as some of the previous research has indicated that the Raman spectral changes are very small in nature and become more perceptible with time (Bulkin et al 1987; Fechner et al 2005; Piccinini et al 2012). Additionally, this experiment was based on the assumption that each gel would retrograde at a relatively uniform rate. This assumption should be tested in future work. Furthermore, application of this method to a model food system should also be examined. The long-term goal of this research is to develop a Raman spectroscopic method for measuring retrogradation in a model food product like white pan bread, but more development is needed.

References

Almeida, M. R., Alves, R. S., Nascimbem, L. B. L. R., Stephani, R., Poppi, R. J., and de Oliveira, L. F. C. 2010. Determination of amylose content in starch using Raman spectroscopy and multivariate calibration analysis. Anal. Bioanal. Chem. 397:2693-2701.

Bulkin, B. J., Kwak, Y., and Dea, I. C. M. 1987. Retrogradation kinetics of waxy-corn and potato starches; a rapid, Raman-spectroscopic study. Carbohydr. Res. 160:95-112.

Donald, A. M. Understanding Starch Structure and Functionality. Pages 156-184 in: Starch in food: Structure, function and applications. A-C. Eliasson, ed. CRC Press: Boca Raton.

Eliasson, A.-C., Larsson, K., Andersson, S., Hyde, S. T., Nesper, R. and von Schnering, H.-G. 1987. On the structure of native starch: an analogue to quartz structure. Starch/Starke 39:147-152.

Fechner, P. M., Wartewig, S., Kleinebudde, P., and Neubert, R. H. H. 2005. Studies of the retrogradation process for various starch gels using Raman spectroscopy. Carbohydr. Res. 340:2563-2568.

Flores-Morales, A., Jiménez-Estrada, M., and Mora-Escobedo, R. 2012. Determination of the structural changes by FT-IR, Raman, and CP/MAS ^{13}C NMR spectroscopy on retrograded starch of maize tortillas. Carbohydr. Polym. 87:61-68.

Gudmundsson, M. 1994. Retrogradation of starch and the role of its components. Thermochim. Acta 246:329-341.

Karim, A. A., Norziah, M. H., and Seow, C. C. 2000. Methods for the study of starch retrogradation. Food Chem. 71:9-36.

Keetels, C. J. A. M., Oostergetel, G. T., and van Vliet, T. 1996. Recrystallization of amylopectin in concentrated starch gels. Carbohydr. Polym. 30: 61-64.

Kim, I.-H., Yeh, A., Zhao, B. L., and Wang, S. S. 1989. Gelatinization kinetics of starch by using Raman spectroscopy. Biotechnol. Prog. 5:172-174.

Kim, J.-O., Kim, W.-S., and Shin, M.-S. 1997. A comparative study on retrogradation of rice starch gels by DSC, X-ray and alpha-amylase methods. Starch/Starke 49:71-75.

Lai, V. M-.F., Lu, S., and Lii, C.-Y. 2000. Molecular characteristics influencing retrogradation of rice amylopectins. Cereal Chem. 77:272-278.

Nara, S., Mori, A., and Komiya, T. 1978. Study on relative crystallinity of moist potato starch. Starch/Starke 30:111-114.

Ratnayke, W. S., and Jackson, D. S. 2008. Thermal behavior of resistant starches RS 2, RS 3, and RS 4. J. Food Sci. 73:C356-C366.

Ribotta, P. D., Cuffini, S., León, A. E., and Añón, M. C. 2004. The staling of bread: an X-ray diffraction study. Eur. Food. Res. Technol. 218:219-223.

Satin, M. 2000. Functional Properties of Starches. FAO Agriculture and Consumer Protection Department: Rome. Available online at: http://www.fao.org/ag/magazine/pdf/starches.pdf

Zeleznak, K. J. and Hoseney, R. C. 1986. The role of water in the retrogradation of wheat starch gels and bread crumb. Cereal Chem. 63:407-411.

Zobel, H. F., and Kulp, K. 1996. The Staling Mechanism. Pages 1-64 in: Baked Goods Freshness: Technology, Evaluation, and Inhibition of Staling. R. E. Hebeda and H. F. Zobel, eds. Marcel Dekker: New York.

SUMMARY

Raman spectroscopy may able to offer an avenue of rapid, non-destructive testing for determining certain quality attributes of starch like amylose-amylopectin ratios of starch. The amylose content of normal/waxy corn starch mixtures was determined using a dual wavelength colorimetric iodine binding method. Partial least-squares regression was used to develop calibration models for measuring amylose content based on the reference data and using Raman spectroscopy. Truncating the spectral region to 2000 to 250 cm^{-1} improved the model results (r^2 of validation = 0.831 for a 7-factor PLS model, SEP = 2.90%). Excluding a cold water swelling starch from the calibration data improved the model results marginally (r^2 of validation = 0.860 for a 5-factor full region PLS model, SEP = 2.70%). The study found that dispersive Raman spectroscopy may not be suited for all purposes of estimating amylose-amylopectin ratios of corn starches; however, the method was easily capable of discriminating between waxy and normal starches, giving it the potential to be used in applications like screening to confirm the identity of starch shipments. Raman spectroscopy's ability to monitor starch retrogradation was also examined.

Though many methods exist for measuring starch retrogradation in food products, few methods could offer the portability and non-destructive capabilities of which Raman spectroscopy is capable. Starch gels were prepared and measured using dispersive Raman spectroscopy. Also, the relative crystallinity of starch gels was measured using X-ray diffraction and calculated using two different methods, and the results were correlated with intensity changes of the Raman band at 480 cm^{-1} calculated using three

different methods. But, no correlation was observed ($r^2 < .1$). The overall noise level of the spectral data and the low concentration of starch used per gel (10% w/v) were implicated as possible causes of the unpredictability of the results seen in both the reference data and the Raman spectral data. Future work should include monitoring starch gels with higher concentration over a longer time period, testing the assumption that starch gels held under similar conditions will retrograde at a relatively uniform rate, followed by extension of any successful method for measuring retrogradation in starch gels to measuring retrogradation in a model food system like white pan bread. The study concluded that applying Raman spectroscopy to measuring starch retrogradation in low concentration starch gels could be problematic.

APPENDIX

Sample No.	% Waxy	% Normal	Starch Blend Code
1	0	100	2
2	0	100	5
3	5	95	3
4	5	95	4
5	5	95	6
6	5	95	2
7	10	90	3
8	10	90	4
9	10	90	1
10	10	90	1
11	15	85	6
12	15	85	2
13	15	85	1
14	15	85	5
15	20	80	5
16	20	80	3
17	20	80	4
18	20	80	5
19	25	75	6
20	25	75	6
21	25	75	2
22	25	75	2
23	30	70	5
24	30	70	2
25	30	70	6
26	30	70	4
27	35	65	4
28	35	65	1
29	35	65	3
30	35	65	2
31	40	60	2
32	40	60	2
33	40	60	4
34	40	60	3
35	45	55	6
36	45	55	1
37	45	55	1
38	45	55	3
39	50	50	1

40	50	50	1
41	50	50	2
42	50	50	3
43	55	45	1
44	55	45	1
45	55	45	3
46	55	45	4
47	60	40	1
48	60	40	1
49	60	40	1
50	60	40	2
51	65	35	2
52	65	35	2
53	65	35	3
54	65	35	2
55	70	30	1
56	70	30	1
57	70	30	2
58	70	30	4
59	75	25	4
60	75	25	2
61	75	25	1
62	75	25	1
63	80	20	1
64	80	20	1
65	80	20	2
66	80	20	3
67	85	15	6
68	85	15	1
69	85	15	3
70	85	15	1
71	90	10	4
72	90	10	4
73	90	10	1
74	90	10	4
75	95	5	2
76	95	5	4

77	95	5	1
78	95	5	2
79	100	0	1
80	100	0	4
81	100	0	6

Table A.1: Mixing protocol for preparation of corn starch mixtures.

Blend Code	Normal Starch	Waxy Starch
1	Argo Normal Corn Starch	National Starch Amioca
2	National Starch MELOJEL	National Starch Amioca
3	Argo Normal Corn Starch	NS&CC Novation 4600
4	National Starch MELOJEL	NS&CC Novation 2600
5	Argo Normal Corn Starch	NS&CC Novation 2600
6	National Starch MELOJEL	NS&CC Novation 4600

Table A.2: Summary of blend codes used for preparation of normal and waxy corn starch mixtures.

RPD Value	Classification	Application
0.0-2.3	Very poor	Not recommended
2.4-3.0	Poor	Very rough screening
3.1-4.9	Fair	Screening
5.0-6.4	Good	Quality control
6.5-8.0	Very good	Process control
8.1+	Excellent	Any application

Table A.3: Classifications and suggested analytical applications of a model based on the ratio of the standard error of prediction to the standard deviation of the validation data. Adapted from Williams (2004).